Mon. Not. R. Astron. Soc. **296,** 1019–1040 (1998)

The formation of double degenerates and related objects

Zhanwen Han[1,2]

[1] *Centre for Astrophysics, University of Science and Technology of China, Hefei, 230026, China*
[2] *Yunnan Observatory, Academia Sinica, Kunming, 650011, China*

Accepted 1998 January 16. Received 1998 January 5; in original form 1997 June 24

ABSTRACT

I systematically investigate the formation of double degenerates (DDs) via binary interactions. I consider three evolutionary channels for their formation [stable Roche lobe overflow (RLOF) plus common envelope (CE), CE plus CE, exposed core plus CE], and carry out Monte Carlo simulations. I explore the effects of model parameters, such as the tidal-enhancement parameter for stellar wind, the mass transfer efficiency for stable RLOF, and the CE ejection efficiency, on my results. I also explore the effects of various assumptions about age, metallicity, mass ratio distribution and wind velocity.

My results show that the model is successful in the explanation of the formation of DDs. I explain satisfactorily the distributions of masses, mass ratios, orbital periods and birth rate of the observed DDs. The main conclusions are the following. (i) Stable RLOF plus CE and CE plus CE are the main evolutionary scenarios leading to the formation of DDs. (ii) The Galactic birth rate of DDs is 0.03 yr^{-1}, and the birth rate of DDs with helium (He) white dwarfs (WDs) as brighter components is 0.017 yr^{-1}. (iii) The number of detectable DDs in our Galaxy is 3×10^6, and DDs with brighter He WDs make up 56 per cent. (iv) The distribution of orbital periods for detectable DDs peaks around 6 h. (v) WD 0957−666 and WD 1101+364 are formed through the stable RLOF plus CE scenario, and WD 0135−052 is possibly a carbon–oxygen (CO) WD pair rather than a helium (He) WD pair. (vi) The Galactic birth rates of close WD binaries and DD mergers are 0.074 and 0.029 yr^{-1}, respectively. (vii) The mergers of two He WDs and the mergers of He and CO WDs have masses of 0.61 ± 0.09 and $0.96 \pm 0.13\,M_\odot$, respectively. (viii) Mass transfer during stable RLOF is not conservative. (ix) A tidally enhanced stellar wind exists.

I also investigate the formation of Type Ia supernovae (SNe Ia), cataclysmic variables (CVs), subdwarf O-type (sdO) stars and R Coronae Borealis (R CrB) stars. The birth rates of SNe Ia and CVs are successfully explained in the above model. The model also shows that CVs with long orbital periods tend to have CO WDs. The birth rates of the mergers of two He WDs (sdO stars) and the mergers of He and CO WDs (R CrB stars) are 0.006 and 0.018 yr^{-1} in the Galaxy, respectively. The birth rates of CVs, DDs, DD mergers and SNe Ia are more sensitive to the recent stellar formation history than to the past one.

Key words: binaries: general – stars: evolution – stars: mass-loss – novae, cataclysmic variables – supernovae: general – white dwarfs.

1 INTRODUCTION

Double degenerates (DDs), which are binaries consisting of two degenerate stars (white dwarfs: WDs), play an important role in stellar evolution as they are possible Type Ia supernova progenitors and contain information about common envelope evolution.

Lots of observational attempts have been made to find DDs during the past decades. Only two DDs, however, had been found (Schulz & Wegner 1981; Saffer, Liebert & Olszewski 1988; Iben & Webbink 1989; Bragaglia et al. 1990) before Marsh, Dhillon & Duck (1995) and Marsh (1995) had a great success. Marsh et al. (1995) observed seven white dwarfs with masses less than $0.45\,M_\odot$ chosen from the 129 DA white dwarfs whose masses were determined by Bergeron, Saffer & Liebert (1992), and they found five DDs. Marsh (1995) found another DD shortly afterwards, Holberg et al. (1995) found one more, and Moran, Marsh & Bragaglia (1997) revised the results on WD 0957−666.

The high success rate of Marsh et al. (1995) comes from their expectation that low-mass white dwarfs may be members of close binaries, since the evolution of a binary system is generally needed

Table 1. Parameters of observational DDs.

DD	WD number	Name	M_1 ($M_\odot$)	M_2 ($M_\odot$) († for lower limit)	Orbital Period (days)	mass ratio $q = M_1/M_2$	References
A	0135−052	L870-2/EG11	0.31	0.35	1.56	0.90	a, b
a			0.54	0.61			c
B	0957−666		0.38	0.33	0.061	1.15 ± 0.10	d,e
C	1101+364	PG 1101+364	0.27	0.31	0.1446	0.87 ± 0.03	f
D	1202+608	GD 314/LB 2197	0.486	0.25†	1.49		g
E	1241−010	PG 1241-010	0.31	0.373†	3.35		h
F	1317+453	G 177-31	0.33	0.421†	4.8		h
G	1713+332	GD 360	0.35	0.178†	1.12		h
H	2032+188	GD 231	0.36		2-10 (6‡)		h
I	2331+290	GD 251	0.39	0.322†	0.14-0.20 (0.17‡)		h

The first column gives a letter representation (A to I) for each DD. Note that both letters 'A' and 'a' represent the same DD, i.e. 0135−052. WD stands for white dwarf, and M_1 and M_2 for the mass of the primary (the brighter component) and the secondary of a DD, respectively. † denotes the figure that is the lower limit of the secondary mass of a DD, and ‡ the figure that is adopted in later plotting. References a to h correspond to a: Saffer et al. 1988; b: Schulz & Wegner 1981; c: Iben & Webbink 1989; d: Bragaglia et al. 1990; e: Moran et al. 1997; f: Marsh (1995); g: Holberg et al. 1995; h: Marsh et al. 1995.

to obtain white dwarfs with masses below 0.45 $M_\odot$. As theoretically pointed out by Han, Podsiadlowski & Eggleton (1994, hereafter HPE1), however, the evolution of a single star of Population I with a zero-age main-sequence mass less than 1.0 $M_\odot$ may also produce low-mass white dwarfs. The white dwarfs in Stein 2051B and 40 Eri B have masses around 0.45 $M_\odot$; both of these white dwarfs are in sufficiently wide orbits (∼350 and 250 yr respectively: van de Kamp 1971) that there should have been no binary interaction in the past. Single star evolution may play a role in these cases.

Han, Podsiadlowski & Eggleton (1995, hereafter HPE2) and Han et al. (1995, hereafter HEPT) carried out several large sets of Monte Carlo simulations, investigating the formation of bipolar planetary nebulae, barium and CH stars, and related binary objects including DDs. The results on DDs were satisfactory at the time of publication of HPE2 and HEPT. Following the recent discovery by Marsh et al. (1995), Marsh (1995) and Holberg et al. (1995), however, I need a more detailed and systematic investigation of the formation of DDs in order to explain their observational properties. I am especially interested in the problem that mass ratios known for DDs are all around 0.9 or 1.1, which has not been explained successfully in previous studies.

A DD system may be coalesced due to gravitational radiation if the system has a short enough period (≲0.2 h). The coalescence may lead to a Type Ia supernova (SN Ia) explosion if the total mass of the system is larger than the Chandrasekhar mass limit (Sparks & Stecher 1974; Iben & Tutukov 1984a; Nomoto & Iben 1985; Webbink & Iben 1987). If the total mass is less than the limit, however, a subdwarf O-type (sdO) star or an R Coronae Borealis (R CrB) star may be formed (Webbink 1984). A good theory has to be successful in the explanation of both DDs and their mergers.

A cataclysmic variable (CV) is a semidetached binary system consisting of a white dwarf (WD) and a main-sequence (MS) star in which mass transfer is stable, or at least fairly stable, on a long timescale. Much theoretical work has been done regarding the production of CVs (Paczyński 1976; Taam, Bodenheimer & Ostriker 1978; Meyer & Meyer-Hofmeister 1979; Livio & Soker 1984, 1988; Taam & Bodenheimer 1989; de Kool 1992; Kolb 1993; HPE2; HEPT; etc). All this work confirms the plausibility of common envelope (CE) evolution (Paczyński 1976) as the best production mechanism. However, CV production and DD production must be closely linked since the production of both CVs and DDs involves CE evolution. A good theory has to account for the statistics of both.

In this paper, I propose possible evolutionary channels for the formation of DDs and related objects (SNe Ia, sdO stars, CVs) in which I investigate the role of interacting binaries. I use a Monte Carlo simulation of a population of 10^5 binaries to make a quantitative study of my model, and to explore the dependence of my results on the assumptions in the model and on the metallicity and age of the population.

In such a population synthesis paper, I have made some simplifications or approximations similar to those in previous studies (Iben & Tutukov 1984a; Yungelson et al. 1994; Pols & Marinus 1994). One may argue that the results in this paper are less accurate than those in detailed stellar evolution studies (e.g. Sarna, Marks & Smith 1996).

The outline of this paper is as follows. In Section 2 I briefly describe the observational data, and in Section 3 evolutionary channels for the formation of DDs and the related objects. In Section 4 I give a description of the adopted stellar models, and in Section 5 I list the theoretical assumptions of my Monte Carlo simulations. In Section 6 I present the results of the simulations, and in Section 7 I discuss the implications of these results. Finally, in Section 8 I give a summary and conclusions.

2 OBSERVATIONAL DATA ON DDs

In Table 1, I list the parameters of the nine currently known DDs from various resources (Saffer et al. 1988; Schulz & Wegner 1981; Iben & Webbink 1989; Bragaglia et al. 1990; Marsh et al. 1995; Marsh 1995; Holberg et al. 1995; Moran et al. 1997). For convenience in this paper, I use a letter from A to I to represent a DD system ('A' and 'a' are used to represent the same DD, i.e. WD 0135−052; it has two sets of masses determined by different people). I list WD numbers for DD systems and their names in columns 2 and 3 respectively, and primary and secondary masses in columns 4 and 5 respectively. To be consistent with observational conventions, I take more luminous (brighter) component as the primary of a DD system. Some of the secondary masses in column 5 are only lower mass limits derived from observations. In column 6 I list the orbital periods or period ranges, and in column 6 the mass ratios known, which are the ratios of primary mass to the secondary one.

3 FORMATION SCENARIOS OF DDs AND RELATED OBJECTS

3.1 The formation of DDs

The evolution of a binary system is much more complicated than that of a single star. A binary system may experience one or two Roche lobe overflows (RLOF), which may result in CE phases, during its evolution. Different binary systems may evolve quite differently, and there may exist many ways to produce DDs. In the present study, however, I only consider the following evolutionary channels.

Note that the primary of a non-DD binary system is defined as the initially more massive component in the current section and following sections, while the primary of a DD system is always defined as the brighter component throughout this paper.

3.1.1 Stable RLOF plus CE

When the primary of a binary system ($8.0 \geq M_1 \geq 0.8\,\mathrm{M}_\odot$) evolves to the Hertzsprung gap or a red giant, it may fill its Roche lobe and mass transfer happens.

In the case of the mass donor (the primary) being a star in the Hertzsprung gap, where the primary has a radiative envelope, the mass transfer is dynamically stable, provided that the mass ratio (primary to secondary) is not too large (van der Linden 1987). The helium core of the primary is left after the stable RLOF and finally becomes a helium (He) or carbon–oxygen (CO) white dwarf. In my calculations, the mass of the helium core is taken as the core mass of a star of the same initial mass at the beginning of the red giant branch, as is supported by the detailed calculations of close binary evolution by van der Linden (1987) and De Greve (1993) for binaries with their primaries more massive than $3\,\mathrm{M}_\odot$. Since the evolutionary behaviour does not differ significantly between stars more massive than $3\,\mathrm{M}_\odot$ and less massive ones, the above approximation should be reasonable. In fact, the core mass is at its lowest value at the beginning of the red giant branch for a star crossing the Hertzsprung gap, as is shown by detailed stellar evolution calculations (Han 1995). Therefore the approximation made here may affect the final masses of WDs produced from this channel (stable RLOF plus CE). That is to say, DDs produced from this channel may have higher secondary masses than that shown in Fig. 7(a) (see Section 7.8).

In the case of the mass donor being a red giant star, where the primary has a deep convective envelope, RLOF may still be dynamically stable, provided that the primary has lost much of its envelope by stellar wind and the mass ratio is down to a critical value. The stable RLOF in this case also leaves a naked helium or carbon–oxygen core as the primary's remnant, which will evolve to a white dwarf later.

The binary evolution in the above two cases leaves a binary system containing a WD and a secondary star which may have accreted some of the primary's envelope mass during the stable RLOF. I assume that the mass lost from the primary during the RLOF is $M_{\rm flow}$, $\alpha_{\rm RLOF}M_{\rm flow}$ is accreted by the secondary, and $(1-\alpha_{\rm RLOF})M_{\rm flow}$ is lost from the binary system, carrying away the same specific orbital angular momentum as pertains to the primary. The change of separation is expressed as (Han 1995)

$$-\mathrm{d}\ln A = 2\mathrm{d}\ln M_2 + 2\alpha_{\rm RLOF}\mathrm{d}\ln M_1 + \mathrm{d}\ln(M_1+M2), \qquad (1)$$

where A is the separation of the binary system, and M_1 and M_2 the mass of the primary and secondary, respectively. In equation (1), I have introduced a mass transfer efficiency for stable RLOF, $\alpha_{\rm RLOF}$, which is around 0.5 as shown by Paczyński & Ziółkowski (1967) and Refsdal, Roth & Weigert (1974). I, however, take $\alpha_{\rm RLOF}$ to be 0.25, 0.5, 0.75 or 1.0 in order to investigate its effects in our simulations.

Equation (1) is derived using the formula for orbital angular momentum and Kepler's law, and without the inclusion of gravitational radiation and magnetic braking. Most of the primaries of binary systems with RLOF that are stable are stars crossing the Hertzsprung gap, where the stellar wind is small. I simply assume that the RLOF takes no time, and the outcome of the RLOF is estimated from the conditions at the beginning of the RLOF. This simplification is also adopted by others (Iben & Tutukov 1984a; de Kool 1992). Therefore stellar wind is not included in equation (1). It is not expected that such an approximation affects the final results much.

The system continues to evolve and the secondary star may fill its Roche lobe as a star in the Hertzsprung gap or red giant branch, and RLOF occurs. In the former case, I assume that a CE forms when the thermal time-scale mass transfer rate, estimated according to the formalism of Rappaport, Verbunt & Joss (1983), exceeds the Eddington accretion rate of the WD. This is only an approximate criterion since the accreting object will start to swell up at an accretion rate which may be substantially less than the Eddington rate (e.g. Nomoto 1982). This does not, however, automatically lead to a CE phase, since the binary may be very efficient in ejecting matter from the system, which can, in principle, prevent the formation of a CE altogether. However, I find in my simulations that the mass transfer rate is generally so large that a CE phase is unavoidable. (The accreting object may become a red giant and its envelope may engulf the WD and the secondary, and a CE may be formed.) In fact, Iben & Tutukov (1984a,b, 1993) also assume that a CE is formed when the secondary of a WD binary system fills its Roche lobe as a star crossing the Hertzsprung gap. In the latter case, the secondary is a red giant and has a deep convective envelope, and a CE phase is more probable than for the former case. Therefore the RLOF for a binary system containing a WD always results in a CE in my calculations, though the true situation may be more complicated than this.

Embedded in the CE are the dense core of the mass donor and a WD. Owing to frictional drag with the envelope, the orbit of the embedded binary decays. A large fraction of the orbital energy that is released in this spiral-in process is deposited into the envelope (Livio & Soker 1988) and the envelope may be ejected when the total deposited orbital energy, $\alpha_{\rm CE}\Delta E_{\rm orb}$, is larger than the envelope binding energy $E_{\rm env}$, i.e.

$$\alpha_{\rm CE}\Delta E_{\rm orb} \geq E_{\rm env}, \qquad (2)$$

where

$$\Delta E_{\rm orb} \simeq \frac{GM_{\rm c}M_{\rm WD}}{2a_{\rm f}} - \frac{G(M_{\rm c}+M_{\rm e})M_{\rm WD}}{2a_{\rm i}}$$

is the orbital energy released in the orbital contraction, and $E_{\rm env}$ is the envelope binding energy at the beginning of the RLOF; here $M_{\rm c}$ and $M_{\rm e}$ are the core mass and envelope mass of the secondary, respectively, $M_{\rm WD}$ is the mass of the WD (the remnant of the original primary), and $a_{\rm i}$ and $a_{\rm f}$ are the initial and final separations, respectively. In equation (2) I have introduced an efficiency parameter $\alpha_{\rm CE}$ to parametrize the uncertainties of the CE ejection process. $\alpha_{\rm CE} \sim 1$ is required for a successful explanation of the formation of bipolar planetary nebulae (HPE2); I, however, take $\alpha_{\rm CE}$ to be 0.5 or 1.0 in this paper in order to investigate its influence. Note that my definition of $\alpha_{\rm CE}$ is similar to that of Webbink (1984)

and de Kool (1990, 1992), but differs substantially from that of Iben & Tutukov (1984a) (see section 6.10.ii of HPE2 for details).

Mass accretion of the WD during the CE phase is ignored in my simulation, since the time-scale for the CE phase is sufficiently small (Livio & Soker 1988).

The ejection of the above CE produces a DD system with a short orbital period.

3.1.2 CE plus CE

When the primary fills its Roche lobe in the Hertzsprung gap or red giant branch, RLOF occurs. If the mass ratio of the primary to the secondary exceeds 3.2 in the case of the mass donor being a Hertzsprung gap star, which has a radiative envelope, RLOF is dynamically unstable according to Eggleton's simple model for the onset of RLOF (Eggleton, private communication). In the case of the mass donor being a red giant star, RLOF is dynamically unstable if the mass ratio is greater than a critical value q_c (Hjellming & Webbink 1987). Webbink (1988) estimates the critical mass ratio, for $M_c \geq 0.2$, as

$$q_c = 0.362 + \frac{1}{3(1 - M_c/M_1)}, \tag{3}$$

where M_c is the mass contained in the donor star's core and M_1 is the mass of the donor star. Equation (3) is derived for conservative evolution and q_c should depend on α_{RLOF} for non-conservative evolution. However, Pastetter & Ritter (1989) find that q_c is only weakly dependent on α_{RLOF}; the actual critical mass ratio is a little bit lower than q_c. Recently, Soberman, Phinney & van den Heuvel (1997) made a comprehensive study of the stability criteria for mass transfer in binary stellar evolution. Their conclusions are in contrdiction to Pastetter & Ritter (1989). Soberman et al. (1997) find that the critical mass ratio is very different for different modes of mass transfer. From their figs 1 and 4, one sees that mass transfer is always dynamically stable (independent of mass ratio) for the isotropic wind mode if the core mass fraction of the donor star is larger than 0.4. The ring formation mode, however, usually has a dynamical instability. The critical mass ratio for the isotropic re-emission mode is higher than for the conservative mode. Also, the critical mass ratio depends heavily on the model parameters of mass transfer (see figs 5, 6 and 7 of Soberman et al. 1997). For simplicity, I take equation (3) to be valid for non-conservative evolution. This approximation may affect the final results of the present study. A higher q_c gives rise to more cases of stable RLOF plus CE and fewer cases of CE plus CE.

Dynamically unstable mass transfer is expected to lead to the formation of a CE (Paczyński 1976), which consists mainly of the material from the envelope of the donor star.

The CE may be ejected if the energy deposited into it during the spiral-in process is large enough (see the above subsection). A WD binary system is thus produced.

The secondary continues to evolve and may experience another RLOF, and the RLOF may also be dynamically or thermally unstable and a CE phase is expected. In fact, however, I always assume that a CE forms for the second RLOF, if the secondary fills its Roche lobe as a star in the Hertzsprung gap or red giant branch, as shown in the above subsection (the sixth paragraph).

Similarly, the ejection of the CE leaves a DD system.

3.1.3 Stable RLOF plus stable RLOF or CE plus stable RLOF

A binary system may experience a stable RLOF or a CE phase when the primary evolves and fills its Roche lobe as a star in the Hertzsprung gap or red giant branch, and the evolution may leave a WD binary system subsequently. The WD binary system may also suffer another RLOF, but the RLOF always results in the formation of a CE in my present study as shown in the above subsections, though this may be debatable (see the sixth paragraph of subsection 3.1.1). Therefore the channels of 'stable RLOF plus stable RLOF' and 'CE plus stable RLOF' for *the formation of DDs* are not considered any more in the following discussions.

3.1.4 Single CE

A binary system may experience an RLOF during its evolution. If, at the RLOF, both components are in the red giant branch (the first red giant branch or the asymptotic giant branch) and the mass ratio of primary to secondary is larger than the critical value given by Webbink (1988), a CE may be formed, containing two degenerate cores. The ejection of the CE may leave a DD system. The possibility of this is quite small and the number of DDs produced this way is only a few per cent of the total DDs (HPE2). This channel is ignored in my present study due to the inability to cope with such a case in my Monte Carlo simulation code for this paper.

3.1.5 Exposed core plus CE

The primary may have lost all its envelope via stellar wind before it fills its Roche lobe in the red giant branch. The core (WD) is exposed and the system becomes a WD binary. The secondary continues to evolve and may fills its Roche lobe as a star in the Hertzsprung gap or the red giant branch. This will result in the formation of a CE. The ejection of the CE may leave a DD system. A DD system produced this way has a longer orbital period than for the case of 'CE plus CE', since the binary system avoids one CE phase.

In brief, the three channels considered for the formation of a DD system in my model are:

(1) stable RLOF + CE;
(2) CE + CE;
(3) exposed core + CE.

I define four types of DDs: He+He, He+CO, CO+He, CO+CO. A DD of He+He type consists of two He WDs, and a DD of CO+CO type consists of two CO WDs. The He+CO or CO+He DD is made of an He WD and a CO WD. If an He WD is produced first and a CO WD second in the above evolutionary channel, the final DD is of CO+He type, otherwise it is of He+CO type. The He WD is the younger component of a DD of He+CO type, while the CO WD is the younger component of the CO+He DD.

3.2 The formation of SNe Ia, sdO stars, R CrB stars and CVs

A DD system loses its orbital angular momentum due to gravitational radiation (Landau & Lifshitz 1962) and this may result in the merger of the system. The wider DDs that have not already coalesced in the past can in principle be observed.

The loss rate of orbital angular momentum due to gravitational radiation (Landau & Lifshitz 1962) is expressed as

$$\frac{\dot{J}_{orb}}{J_{orb}} = -8.30 \times 10^{-10} \left(\frac{M_1}{M_\odot}\right) \left(\frac{M_2}{M_\odot}\right) \left(\frac{M_1 + M_2}{M_\odot}\right) \left(\frac{A}{R_\odot}\right)^{-4} \mathrm{yr}^{-1}, \tag{4}$$

where J_{orb} is the orbital angular momentum, and M_1 and M_2 are the masses of the primary and secondary of a DD system. A is the separation and the time is in years.

A Type Ia supernova (SN Ia) explosion may happen as a result of a CO+CO DD merger if the total mass is larger than the Chandrasekhar limit (Sparks & Stecher 1974; Iben & Tutukov 1984a, etc). The accretion of hydrogen on to a white dwarf via RLOF, from a subgiant donor, may also produce a SN Ia if the mass of the white dwarf grows towards the Chandrasekhar limit (e.g. Della Valle & Livio 1996), but this is, however, beyond the scope of this paper. In the present study, I only consider the former case, i.e. the classical SN Ia model.

As pointed out by Webbink (1984), the coalescence of an He+He DD may finally lift its degeneracy, burning helium in a region of the Hertzsprung–Russell (HR) diagram occupied observationally by the sdO stars (Greenstein & Sargent 1974; Wesemael et al. 1982). The coalescence of an He+CO or an CO+He DD may result in the formation of an R CrB star (Webbink 1984).

When a binary evolves, the primary (by definition here, the *initially* more massive component) expands and may fill its Roche lobe as a star in the first giant branch (FGB) or the asymptotic giant branch (AGB). If the RLOF is dynamically unstable, the binary is expected to suffer CE evolution, and the binary may become a short-period system, composed of a WD and an MS star. The system may even coalesce in some cases. If the period of the post-CE system is short enough ($\lesssim 1-2$ d), the system suffers orbital angular momentum loss due to magnetic braking (Eggleton 1976; Verbunt & Zwaan 1981) in some cases and gravitational wave radiation (e.g. Landau & Lifshitz 1962), and may become a semidetached system. If the mass transfer in the semidetached system is stable, a CV is formed. I adopt the formalism devised by de Kool (1992) for my simulations (see HPE2 for a more detailed description). If the mass transfer is thermally unstable, an ultrasoft X-ray source may be formed (e.g. van den Heuvel et al. 1992). I do not study the formation of the source, however, in the present study since this paper is mainly concerned with DDs.

Note that gravitational radiation or magnetic braking is considered only for the evolution of DDs or the formation of CVs, i.e. in the current subsection. They are not considered for other systems or other evolutionary stages.

4 STELLAR MODELS

In order to follow the evolution of individual sample stars in a Monte Carlo simulation, I need sets of stellar evolution models from which the required stellar properties can be extracted. In this section, I briefly describe the stellar evolution models, the stellar wind problem, the method for calculating the envelope energy, the initial–final mass relation, and the evolution of DDs.

4.1 Stellar model grid

With Eggleton's stellar evolution code (Eggleton 1971, 1972, 1973; Eggleton, Faulkner & Flannery 1973; HPE1), and the latest opacity tables of Rogers & Iglesias (1992), supplemented with molecular opacities at low temperatures from the compilation of Weiss, Keady & Magee (1990), I construct a grid of stellar evolutionary models for two compositions, a typical Population I (Pop I) composition with hydrogen abundance $X = 0.70$, helium abundance $Y = 0.28$ and metallicity $Z = 0.02$, and a representative Population II (Pop II) composition with $X = 0.75$, $Y = 0.25$ and $Z = 0.001$. For a detailed description of the evolutionary computational method, see HPE1. The models do not include mass loss, and the stellar wind is included afterwards explicitly using a Runge–Kutta integration method. The model uses a ratio of mixing length to pressure scaleheight $\alpha = 2$, which gives a roughly correct lower MS, as determined observationally by Andersen (1991). The models well reproduce the location of the red giant branch in the HR diagram for stars in the Hyades supercluster (Eggen 1985), as determined by Bessell et al (1989). The model grid for Pop I covers the range from 0.8 to 16.0 $M_\odot$ at roughly equal intervals in $\log M$ ($M = 0.8$, 1.0, 1.25, 1.60, 2.0, 2.5, 3.0, 4.0, 5.0, 6.3, 8.0, 10.0, 12.5 and 16.0 $M_\odot$). The Pop II model grid is the same but only goes up to 8 $M_\odot$. The stellar parameters required in the Monte Carlo simulations are stored at somewhat more than 50 points for each evolutionary track in the HR diagram. To determine the required stellar parameters between grid points, I have devised an interpolation scheme which yields, with reasonable precision, the stellar age, radius, effective temperature, surface luminosity, core mass, core radius, envelope gravitational binding energy and envelope thermal energy.

4.2 Stellar wind

I include stellar wind explicitly in the interpolation code for the stellar model grids, using an adaptive stepsize controlled Runge–Kutta method.

I assume that the stellar wind mass-loss rate of a component (star 1) in a binary system is increased by the presence of its companion star (star 2). The tidal enhancement of mass-loss rate $\dot{M}_1$ of star 1 is modelled by Reimers' (1975) formula with an extra tidal term by Tout & Eggleton (1988):

$$\dot{M}_1 = -4\times 10^{-13}\frac{R_1 L_1}{M_1}\left\{1 + B\times \min\left[\left(\frac{R_1}{R_{\rm L1}}\right)^6, \frac{1}{2^6}\right]\right\}, \qquad (5)$$

where R_1, L_1 and M_1 are stellar radius, luminosity and mass in solar units, respectively; and the time is in yr. $R_{\rm L1}$ is the radius of the Roche lobe around star 1. B is more than 3000 in Tout & Eggleton's model (1988), and is 10 000 in the wind-driven mass transfer theory of Tout & Hall (1991), which means that the mass-loss rate $|\dot{M}_1|$ could be 150 times as large as Reimers' rate when the star nearly fills its Roche lobe. However, in my calculation I take 0, 500, 1000, 2000, 4000, 10 000 for B, in order to investigate the effects of such tidally enhanced stellar winds. A simulation without any stellar wind is also carried out for comparison purposes.

Some of the mass lost in the form of stellar wind from star 1 may be accreted by star 2. The mass accretion rate is expressed by Boffin & Jorrissen (1988) as

$$\dot{M}_2 = -\frac{1}{\sqrt{1-e^2}}\left(\frac{GM_2}{V_{\rm wind}^2}\right)^2 \frac{\alpha_{\rm acc}\dot{M}_1}{2a^2(1+V_{\rm orb}^2/V_{\rm wind}^2)^{3/2}}, \qquad (6)$$

where $V_{\rm orb} = \sqrt{G(M_1+M_2)/a}$ is the orbital velocity; G is the gravitational constant; M_1, M_2 and a are the masses of stars 1 and 2, and the orbital separation (semimajor axis), respectively; e is the orbital eccentricity; $\alpha_{\rm acc}$ is the accretion efficiency parameter; and $V_{\rm wind}$ is the velocity of the wind. I take e as 0.23, which is the average orbital eccentricity for red giant binaries (Boffin, Paulus & Cerf 1992), since mass is lost via stellar wind mainly in the red giant phase. I take the accretion efficiency parameter $\alpha_{\rm acc}$ to be 1.5 (Boffin, Cerf & Paulus 1993), which is appropriate for Bondi–Hoyle accretion. In most of my simulations, the stellar wind velocity $V_{\rm wind}$ is taken to be 20 km s^{-1}; I also take $V_{\rm wind} = 10$ and 40 km s^{-1} for comparison purposes. The velocity of the superwind (starting at the end of AGB evolution of a single star) is taken to be 10 km s^{-1} (Kwok 1982; Pottasch 1984).

Any accretion on to a white dwarf is, however, not considered in my present study. Mass accretion on to a white dwarf is quite

complicated. As shown by Shara, Prialnik & Kovetz (1993), WDs, accreting hydrogen-rich matter, undergo periodic eruptions. A carbon–oxygen WD may eject the entire accreted matter while a helium white dwarf retains some of the accreted material which is added to the core after being burnt into helium. Prialnik & Kovetz (1995) show that accretion at rates $\dot{M} \geq 10^{-7}\,\mathrm{M_\odot yr^{-1}}$ invariably increase the mass of an accreting white dwarf. For accretion rates $\dot{M} \leq 10^{-9}\,\mathrm{M_\odot yr^{-1}}$, the mass decreases under all circumstances. For accretion rates around $10^{-8}\,\mathrm{M_\odot yr^{-1}}$, the fate of the WD is determined by its temperature. The envelope of the accreting WD expands and may engulf its companion star, and may form a CE. This is, however, not taken into account in the above mass accretion studies. The above work is still progressing (Kovetz & Prialnik 1997). Anyway, I simply assume that the mass of a WD remains unchanged after birth. This assumption is similar to that by Iben, Tutukov & Yungelson (1997).

The mass lost via stellar wind from star 1, excluding that accreted on to star 2, leaves the binary system, and is assumed to carry away the same specific orbital angular momentum as pertains to star 1.

4.3 Envelope energy

The envelope binding energy $E_{\rm env}$ is required in the criterion for CE ejection. I take it as

$$E_{\rm env} = E_{\rm gr} - \alpha_{\rm th}E_{\rm th} = \int_{M_{\rm c}}^{M_{\rm s}} \frac{Gm}{r}\mathrm{d}m - \alpha_{\rm th}\int_{M_{\rm c}}^{M_{\rm s}} U\mathrm{d}m, \qquad (7)$$

where the envelope energy consists of two parts, the gravitational binding energy $E_{\rm gr}$ and the thermal energy $E_{\rm th}$, $M_{\rm s}$ is the stellar surface mass and $M_{\rm c}$ the core mass. For practical determination of $M_{\rm c}$, see section 2 of HPE1. U is the internal energy of thermodynamics, involving terms due to the ionization of H and He and the dissociation of H_2, as well as the basic $3\Re T/2\mu$ for a simple perfect gas. The thermal energy contribution parameter $\alpha_{\rm th}$ is taken to be 1 (HPE2)

4.4 Initial–final mass relation

When a single star or the primary of a wide binary evolves to the AGB phase, the envelope is assumed to be ejected in the form of a superwind (a slow but copious wind) when the core mass of the AGB star reaches the final mass given by the initial–final mass relation of HPE1:

$$\begin{aligned} M_{\rm f} &= \max[0.054 + 0.042M_{\rm i}, \\ &\quad \min(0.36 + 0.104M_{\rm i}, 0.58 + 0.061M_{\rm i})], \\ &\quad 0.8 \leq M_{\rm i} \leq 8\,\mathrm{M_\odot} \end{aligned} \qquad (8)$$

for Population I, and

$$\begin{aligned} M_{\rm f} &= \max[0.54 + 0.073M_{\rm i}, \\ &\quad \min(0.29 + 0.178M_{\rm i}, 0.65 + 0.062M_{\rm i})], \\ &\quad 0.8 \leq M_{\rm i} \leq 7\,\mathrm{M_\odot} \end{aligned} \qquad (9)$$

for Population II, where $M_{\rm i}$ and $M_{\rm f}$ are the initial and final masses of a star in solar masses.

4.5 The evolution of DDs

A DD system loses its orbital angular momentum due to gravitational radiation (Landau & Lifshitz 1962) and the orbit shrinks. DDs with short orbital periods may coalesce as a result of gravitational radiation and may produce SNe Ia or sdO stars or R CrB stars. The wider DDs that have not already coalesced in the past can in principle be observed.

To be consistent with observational conventions, I take the more luminous (brighter) component as the primary of a DD system. It is, however, not easy to determine which component is brighter. As shown in Section 3, a binary system may produce in some way a WD first and the system becomes a WD binary system. The WD binary system may suffer a CE evolution and produce another WD, and lead to the formation of a DD system. A WD cools after being produced and the cooling rate is dependent on its mass and composition. On the other hand, the WD produced first may be rejuvenated during the CE evolution, producing the DD system. A comprehensive model for the cooling and rejuvenation of WDs is not available to my knowledge, though lots of work on WD evolution have been done in the past (Winget 1987; Iben, Fujimoto & MacDonald 1992; Shara et al. 1993; Castellani, Degl'Innocenti & Romaniello 1994; Althaus & Benvenuto 1997). In my present study, I simply take the younger WD, which is produced second during a binary evolution, as the brighter one, and the older WD, which is produced first, as the dimmer one.

The lifetime of a WD in a 'detectable' state is assumed to be 10^8 yr or shorter (if the components of a system merge in less than 10^8 yr) since most WD observed in close binaries have cooled for about 10^8 yr or less. This assumption is similar to that by Iben et al. (1997). A rejuvenation model, which is not available, is needed to determine the liefetime of a DD with both components being detectable.

5 MONTE CARLO SIMULATION PARAMETERS

To estimate the importance of each evolutionary channel for the production of DDs, I have performed a series of Monte Carlo simulations. In each simulation, I follow the evolution of 1×10^5 sample binaries according to my grids of stellar models. In addition, the simulations require as input the star formation rate (SFR), the initial mass function (IMF) of the primary, the initial mass ratio distribution, and the distribution of initial orbital separations.

(1) The SFR is taken to be constant over the last 15 Gyr.

(2) A simple approximation to the IMF of Miller & Scalo (1979) is used; the primary mass is generated with the formula of Eggleton, Fitchett & Tout (1989),

$$M_1 = \frac{0.19X}{(1-X)^{0.75} + 0.032(1-X)^{0.25}}, \qquad (10)$$

where X is a random number uniformly distributed between 0 and 1. The adopted ranges of primary masses are 0.8 to 8.0 $\mathrm{M_\odot}$ for Pop I, and 0.8 to 7.0 $\mathrm{M_\odot}$ for Pop II. The latest study of the IMF by Kroupa, Tout & Gilmore (1993) supports this IMF.

(3) The mass ratio distribution is quite controversial. I mainly take a constant mass ratio distribution (Mazeh et al. 1992; Goldberg & Mazeh 1994),

$$n(q) = 1, \qquad 0 \leq q \leq 1, \qquad (11)$$

where $q = M_2/M_1$. In order to study the influence of the mass ratio distribution, I also take a distribution where both components are chosen randomly and independently from the same IMF (equation 10).

(4) I assume that all stars are members of binary systems, and that the distribution of separations is constant in $\log a$ (a is the

Table 2. Birth rates (yr^{-1}) of DDs from different channels and birth rates of various types of DDs in the Galaxy.

Model set	Pop	Stellar wind	B	$\alpha_{\rm RLOF}$	$n(q)$	$\alpha_{\rm CE}$	$V_{\rm wind}$ ($km\,s^{-1}$)	Age (Gyr)	RLOF + CE	CE + CE	Exposed core+ CE	He +He DD	He +CO DD	CO +He DD	CO +CO DD	Total DD
1	I	No	0	0.5	(a)	1.0	20	15-0	0.0082	0.0238	0.0000	0.0120	0.0123	0.0033	0.0044	0.0320
2	I	Yes	0	0.5	(a)	1.0	20	15-0	0.0095	0.0263	0.0000	0.0140	0.0125	0.0042	0.0052	0.0358
3	I	Yes	500	0.5	(a)	1.0	20	15-0	0.0118	0.0176	0.0002	0.0072	0.0116	0.0052	0.0055	0.0296
4	I	Yes	1000	0.5	(a)	1.0	20	15-0	0.0139	0.0144	0.0017	0.0061	0.0108	0.0074	0.0057	0.0300
5	I	Yes	2000	0.5	(a)	1.0	20	15-0	0.0157	0.0106	0.0048	0.0059	0.0088	0.0104	0.0061	0.0311
6	I	Yes	4000	0.5	(a)	1.0	20	15-0	0.0144	0.0082	0.0075	0.0044	0.0071	0.0126	0.0059	0.0301
7	I	Yes	10000	0.5	(a)	1.0	20	15-0	0.0108	0.0057	0.0104	0.0032	0.0051	0.0135	0.0050	0.0269
8	I	Yes	1000	0.25	(a)	1.0	20	15-0	0.0132	0.0145	0.0018	0.0075	0.0113	0.0047	0.0060	0.0295
9	I	Yes	1000	0.75	(a)	1.0	20	15-0	0.0155	0.0145	0.0018	0.0052	0.0108	0.0106	0.0051	0.0318
10	I	Yes	1000	1.0	(a)	1.0	20	15-0	0.0165	0.0145	0.0018	0.0053	0.0108	0.0129	0.0039	0.0328
11	I	Yes	1000	0.5	(b)	1.0	20	15-0	0.0018	0.0028	0.0003	0.0017	0.0019	0.0008	0.0004	0.0048
12	I	Yes	1000	0.5	(a)	0.5	20	15-0	0.0106	0.0087	0.0018	0.0023	0.0072	0.0070	0.0045	0.0211
13	I	Yes	1000	0.5	(a)	1.0	10	15-0	0.0147	0.0150	0.0019	0.0066	0.0109	0.0082	0.0059	0.0315
14	I	Yes	1000	0.5	(a)	1.0	40	15-0	0.0130	0.0142	0.0002	0.0059	0.0108	0.0053	0.0054	0.0274
15	I	Yes	1000	0.5	(a)	1.0	20	10-0	0.0137	0.0128	0.0016	0.0052	0.0099	0.0074	0.0057	0.0281
16	II	Yes	1000	0.5	(a)	1.0	20	15-0	0.0328	0.0157	0.0076	0.0182	0.0124	0.0165	0.0091	0.0561
17	II	Yes	1000	0.5	(a)	1.0	20	15-10	0.0020	0.0013	0.0015	0.0027	0.0008	0.0012	0.0002	0.0048

The simulations assume an IMF similar to that of Miller & Scalo (1979), and that 50 per cent of all stellar systems are binaries with orbital periods less than 100 yr. I also assume that one binary with $M_1 \geq 0.8\,M_\odot$ is formed annually in our Galaxy (e.g. Iben & Tutukov 1984a; Yungelson et al. 1993). The second column (Pop) indicates whether a row is for Pop I or Pop II, the third column (Stellar wind) shows whether stellar wind is considered or not for a row. The fourth column (B) gives the tidal enhancement parameter of the stellar wind. The fifth column ($\alpha_{\rm RLOF}$) is the mass transfer efficiency of stable RLOF, and the sixth column [$n(q)$] is mass ratio distribution, in which (a) stands for a constant distribution (equation 11) and (b) for a distribution where the masses of both components are chosen randomly and independently from the same IMF (equation 10). Column 7 ($\alpha_{\rm CE}$) and 8 ($V_{\rm wind}$) list the ejection efficiency parameter of a CE and the stellar wind velocity in $km\,s^{-1}$ adopted. Column 9 (Age) gives the age range (Gyr; beginning-end). Columns 10–12 list the frequency (yr^{-1}) of DDs from each evolutionary channel (stable RLOF plus CE, CE plus CE, exposed core plus CE). Columns 13–16 list the frequency of various types of DDs (He+He DD, He+CO DD, CO+He DD, CO+CO DD), and the last column lists the total frequency of DDs in the Galaxy.

separation) for wide binaries and falls off smoothly at small separations:

$$an(a) = \begin{cases} \alpha_{\rm sep}(\frac{a}{a_0})^m, & a \leq a_0; \\ \alpha_{\rm sep}, & a_0 < a < a_1, \end{cases} \qquad (12)$$

where $\alpha_{\rm sep} \approx 0.070$, $a_0 = 10\,R_\odot$, $a_1 = 5.75 \times 10^6\,R_\odot = 0.13\,pc$, and $m \approx 1.2$. This distribution implies that there is an equal number of wide binary systems per logarithmic interval, and that approximately 50 per cent of stellar systems are binary systems with orbital periods less than 100 yr.

6 RESULTS

Altogether, I performed 17 sets of calculations with different values for metallicity, wind tidal enhancement parameter B, mass transfer efficiency $\alpha_{\rm RLOF}$ for stable RLOF, mass ratio distribution, CE ejection efficiency, wind velocity, and population age.

The results of these calculations are shown in Table 2, where I list the birth rate (rate of production in yr^{-1}) of DDs for each evolutionary channel and the birth rate for various types of DDs in our Galaxy, assuming that one binary with $M_1 \geq 0.8\,M_\odot$ is formed annually in our Galaxy (e.g. Iben & Tutukov 1984a; Yungelson, Tutukov & Livio 1993) for both Pop I and Pop II. This formation rate is no doubt higher than the real one for Pop II, but the results of this paper can be scaled down for Pop II as required.

I have also made a conversion from the birth rate of DDs to the total number of them, whether presently detectable or not, and the number of DDs with their brighter components detectable at present in the Galaxy, by adopting a constant SFR during the age range (the 9th column in the table). In Table 3, I give the percentage contribution of each evolutionary channel to the total number or the detectable number, and the percentage of various types of DDs. 'Detectable DDs' are defined here as the DDs with their brighter components detectable, i.e. their brighter components have a cooling time of less than 10^8 yr (Iben et al. 1997).

In Table 4, I list the birth rates of post-CE systems (WD binaries), CVs, DD mergers, SNe Ia, the mergers of two He WDs (sdO stars), the mergers of He and CO WDs (R CrB stars), and the mergers of two CO WDs.

I also plot distributions of different properties for detectable DDs, and those for WD binaries and CVs in the Galaxy, in Figs 1–7.

7 DISCUSSION

7.1 The importance of individual evolutionary channels

From Tables 2 and 3, we see that the channels of *stable RLOF plus CE* and *CE plus CE* play the most important role for the formation of DDs. Stable RLOF plus CE is an important channel; it accounts possibly for up to 50 per cent of detectable DDs. CE plus CE is a major channel; up to 74 per cent of detectable DDs may be produced from this channel. *Exposed core plus CE* is a minor channel; it contributes significantly only for very big tidal enhancement parameters $B \geq 2000$, i.e. for binary evolution with a strongly tidally enhanced stellar wind.

7.2 The influence of model parameters

The most influential parameter is that for tidal enhancement of the stellar wind (B). B does not greatly affect the total number of detectable DDs; it does, however, significantly affect the contribution fraction of each evolutionary channel to the detectable DDs and

Table 3. Percentages of DDs from different channels and percentages of various types of DDs at the present time in the Galaxy.

Model set	Pop	Stellar wind	B	$\alpha_{\rm RLOF}$	$n(q)$	$\alpha_{\rm CE}$	$V_{\rm wind}$ (km·s^{-1})	Age (Gyr)	RLOF + CE	CE + CE	Exposed core+ CE	He +He DD	He +CO DD	CO +He DD	CO +CO DD	Total DD
1	I	No	0	0.5	(a)	1.0	20	15-0	27.70	72.30	0.00	17.28	45.94	6.63	30.15	1.042×10^{8}
									25.59	74.41	0.00	37.32	38.50	10.39	13.79	3.205×10^{6}
2	I	Yes	0	0.5	(a)	1.0	20	15-0	30.70	69.30	0.00	16.27	42.09	10.52	31.12	1.331×10^{8}
									26.54	73.46	0.00	39.06	34.79	11.74	14.42	3.579×10^{6}
3	I	Yes	500	0.5	(a)	1.0	20	15-0	44.23	55.38	0.39	4.15	40.54	17.41	37.90	1.399×10^{8}
									39.78	59.54	0.68	24.42	39.24	17.70	18.64	2.961×10^{6}
4	I	Yes	1000	0.5	(a)	1.0	20	15-0	52.65	41.30	6.05	2.55	30.68	31.96	34.80	1.762×10^{8}
									46.17	48.04	5.79	20.41	36.05	24.57	18.97	3.004×10^{6}
5	I	Yes	2000	0.5	(a)	1.0	20	15-0	58.94	24.89	16.17	4.94	18.44	44.79	31.83	2.378×10^{8}
									50.40	34.16	15.44	18.88	28.21	33.39	19.52	3.109×10^{6}
6	I	Yes	4000	0.5	(a)	1.0	20	15-0	59.28	15.56	25.16	7.26	11.78	53.56	27.40	2.657×10^{8}
									47.86	27.24	24.91	14.73	23.74	41.84	19.69	3.007×10^{6}
7	I	Yes	10000	0.5	(a)	1.0	20	15-0	51.57	9.29	39.14	8.21	6.71	62.01	23.06	2.563×10^{8}
									40.02	21.18	38.79	11.80	19.06	50.41	18.73	2.686×10^{6}
8	I	Yes	1000	0.25	(a)	1.0	20	15-0	52.92	40.89	6.19	7.73	31.16	23.51	37.60	1.778×10^{8}
									44.70	49.17	6.13	25.52	38.38	15.97	20.14	2.955×10^{6}
9	I	Yes	1000	0.75	(a)	1.0	20	15-0	57.05	37.84	5.10	3.35	27.94	40.72	27.99	1.999×10^{8}
									48.65	45.66	5.69	16.47	33.97	33.47	16.09	3.182×10^{6}
10	I	Yes	1000	1.0	(a)	1.0	20	15-0	64.19	31.13	4.68	4.87	22.68	52.48	19.98	2.403×10^{8}
									50.24	44.24	5.51	16.05	32.89	39.16	11.91	3.284×10^{6}
11	I	Yes	1000	0.5	(b)	1.0	20	15-0	42.82	44.31	12.87	7.92	37.62	36.14	18.32	2.020×10^{7}
									36.44	57.14	6.42	34.37	40.37	16.98	8.28	4.830×10^{5}
12	I	Yes	1000	0.5	(a)	0.5	20	15-0	49.61	37.67	12.72	1.75	32.85	40.27	25.14	8.295×10^{7}
									50.43	41.00	8.58	11.04	34.08	33.36	21.52	2.110×10^{6}
13	I	Yes	1000	0.5	(a)	1.0	10	15-0	55.68	39.81	4.51	3.63	29.10	33.00	34.27	1.885×10^{8}
									46.53	47.51	5.96	20.93	34.57	25.88	18.62	3.153×10^{6}
14	I	Yes	1000	0.5	(a)	1.0	40	15-0	52.15	47.56	0.29	3.46	35.07	23.03	38.43	1.546×10^{8}
									47.43	51.95	0.62	21.42	39.51	19.34	19.74	2.741×10^{6}
15	I	Yes	1000	0.5	(a)	1.0	20	10-0	58.88	37.90	3.22	3.31	27.38	32.43	36.88	1.180×10^{8}
									48.77	45.64	5.59	18.50	35.08	26.22	20.21	2.811×10^{6}
16	II	Yes	1000	0.5	(a)	1.0	20	15-0	57.59	25.33	17.08	17.96	19.22	38.48	24.34	3.764×10^{8}
									58.49	27.98	13.53	32.38	22.11	29.33	16.17	5.608×10^{6}
17	II	Yes	1000	0.5	(a)	1.0	20	15-10	52.05	24.52	23.43	18.48	19.11	41.20	21.22	1.424×10^{8}
									41.12	27.69	31.20	55.37	17.15	23.76	3.72	4.840×10^{5}

As Table 2, but I list percentages of DDs from different evolutionary channels and for various types of DDs, and the total number of DDs at present in the Galaxy. The percentages and total numbers are obtained by assuming a constant SFR, and DDs suffer from orbital angular momentum loss due to gravitational radiation (Landau & Lifshitz 1962). DDs in this table are the ones that have not been merged in the past, which can in principle be observed. For each model set, two rows are given. The first row is for all the DDs at present, but the second row is for the DDs with a presently detectable component (i.e., the WD produced second during binary evolution is detectable in 10^8 yr from the formation of the DD: e.g. Iben et al. 1997).

the percentage of various types of them. When B increases from 0 to 10 000 (simulation set 2 to 7), the contribution fraction of stable RLOF plus CE to the total detectable DDs increases first from 27 per cent, reaches a maximum of 50 per cent at $B = 2000$, and then decreases to 40 per cent at $B = 10\,000$. When B increases from 0 to 10 000, the fraction of CE plus CE decreases from 73 to 21 per cent, and the fraction of exposed core plus CE increases from 0 to 39 per cent. This could be explained as follows. A larger B means a stronger stellar wind; a star (star 1) loses more mass before it fills its Roche lobe, and the RLOF is more probably dynamically stable, therefore stable RLOF plus CE is more probable and CE plus CE is less probable. A much larger B leads to a much stronger stellar wind, and more stars lose their envelopes via stellar wind before the end of the AGB phase, therefore the number of RLOFs becomes smaller and the number of exposed core plus CEs becomes bigger. The increase in B results in a sharp decrease of the number of detectable He+He DDs (from 39 to 12 per cent), a sharp increase of the number of CO+He DDs (from 12 to 50 per cent), and an increase then a decrease in the number of He+CO and CO+CO DDs. A larger B leads to more stable RLOFs and core exposures for original binary systems. Stable RLOFs and core exposures produce WD binaries with longer orbital periods, while CE evolution tends to produce WD binaries with shorter orbital periods. The secondaries (star 2) of the WD binaries with longer orbital periods may evolve and more probably fill their Roche lobes in the AGB phase than the binaries with shorter orbital periods. CE evolutions with Roche lobe filling stars in the AGB phase may produce CO+He or CO+CO DDs. Therefore a larger B results in the formation of more WD binaries with longer orbital periods, and then more CO+He DDs and fewer He+He DDs.

The mass transfer efficiency parameter of stable RLOF, $\alpha_{\rm RLOF}$, is not an important one in terms of how it affects the fractions of each evolutionary channel and the total numbers of detectable DDs. It does however, affect very much the distribution of mass ratios of detectable DDs. From Tables 2 and 3, we see that an increase in $\alpha_{\rm RLOF}$ leads to a slight increase of the fraction of stable RLOF plus CE. This is because a larger $\alpha_{\rm RLOF}$ gives rise to a more massive secondary after the stable RLOF, and a more massive secondary

Table 4. Birth rates (yr^{-1}) of WD binaries, CVs, DD Mergers, SNe Ia, mergers of two He WD (sdO stars), mergers of He WD with CO WD (R CrB stars), and mergers of two CO WDs in the Galaxy.

Model set	Pop	Stellar wind	B	$\alpha_{\rm RLOF}$	$n(q)$	$\alpha_{\rm CE}$	$V_{\rm wind}$ ($\rm km{\cdot}s^{-1}$)	Age (Gyr)	WD binary	CV	DD Merger	SN Ia	He&He WD Merger (sdO)	He&CO WD Merger (R CrB)	CO&CO WD Merger
1	I	No	0	0.5	(a)	1.0	20	15-0	0.1199	0.0039	0.0310	0.0029	0.0112	0.0154	0.0044
2	I	Yes	0	0.5	(a)	1.0	20	15-0	0.1167	0.0035	0.0354	0.0033	0.0137	0.0166	0.0052
3	I	Yes	500	0.5	(a)	1.0	20	15-0	0.0863	0.0033	0.0291	0.0036	0.0069	0.0167	0.0055
4	I	Yes	1000	0.5	(a)	1.0	20	15-0	0.0742	0.0031	0.0294	0.0036	0.0057	0.0181	0.0057
5	I	Yes	2000	0.5	(a)	1.0	20	15-0	0.0615	0.0029	0.0303	0.0037	0.0054	0.0189	0.0061
6	I	Yes	4000	0.5	(a)	1.0	20	15-0	0.0495	0.0021	0.0293	0.0031	0.0038	0.0196	0.0059
7	I	Yes	10000	0.5	(a)	1.0	20	15-0	0.0379	0.0012	0.0258	0.0023	0.0023	0.0185	0.0050
8	I	Yes	1000	0.25	(a)	1.0	20	15-0	0.0743	0.0033	0.0289	0.0033	0.0070	0.0159	0.0060
9	I	Yes	1000	0.75	(a)	1.0	20	15-0	0.0743	0.0030	0.0313	0.0039	0.0049	0.0213	0.0051
10	I	Yes	1000	1.0	(a)	1.0	20	15-0	0.0743	0.0030	0.0321	0.0031	0.0047	0.0235	0.0039
11	I	Yes	1000	0.5	(b)	1.0	20	15-0	0.0816	0.0155	0.0047	0.0002	0.0016	0.0027	0.0004
12	I	Yes	1000	0.5	(a)	0.5	20	15-0	0.0557	0.0026	0.0205	0.0028	0.0019	0.0141	0.0045
13	I	Yes	1000	0.5	(a)	1.0	10	15-0	0.0800	0.0030	0.0309	0.0037	0.0062	0.0189	0.0059
14	I	Yes	1000	0.5	(a)	1.0	40	15-0	0.0708	0.0031	0.0269	0.0034	0.0054	0.0161	0.0054
15	I	Yes	1000	0.5	(a)	1.0	20	10-0	0.0691	0.0027	0.0281	0.0036	0.0052	0.0172	0.0057
16	II	Yes	1000	0.5	(a)	1.0	20	15-0	0.0847	0.0047	0.0553	0.0077	0.0177	0.0286	0.0091
17	II	Yes	1000	0.5	(a)	1.0	20	15-10	0.0079	0.0007	0.0041	0.0000	0.0022	0.0017	0.0002

Birth rates (frequencies) for various types of systems (events) per year in our Galaxy for the simulations in Table 2. The figures assume that one binary with $M_1 \geq 0.8\,{\rm M}_\odot$ is formed annually in our Galaxy (e.g. Iben & Tutukov 1984a; Yungelson et al. 1993). The SN Ia frequency assumes that Type Ia supernovae result from the merger of two CO WDs with a total mass larger than the Chandrasekhar mass. The last three columns give the frequencies for the merger of two helium WDs (sdO stars), the merger of helium WDs with carbon-oxygen WDs (R CrB stars), and the merger of two carbon-oxygen WDs. The birth rates/frequencies can be approximately converted into local birth rates/frequencies (in units of $\rm pc^{-3}yr^{-1}$) by multiplying them by a factor of 2×10^{-12} $\rm pc^{-3}$. The number of WD binary systems (post-CE systems) whose WD components are detectable is given by the birth rate times 10^8 yr.

evolves more quickly and has a larger final radius, and thus has a greater chance to experience CE evolution, which may produce a DD. Table 2 shows that a larger $\alpha_{\rm RLOF}$ gives a bigger birth rate of CO+He DDs. As seen from Fig. 1, in which I plot the detectable DDs of He+He and CO+CO types in the plane of mass ratio–orbital period for simulation sets 1 to 16, an increase of $\alpha_{\rm RLOF}$ leads to an increase in the mass ratios of DDs ($M_{\rm brighter}/M_{\rm dimmer}$) produced through the channel of stable RLOF plus CE. This is due to the fact that a larger $\alpha_{\rm RLOF}$ results in a more massive secondary after the stable RLOF, and a more massive secondary tends to leave a more massive core as its remnant after the CE phase.

The mass ratio distribution is a very important parameter. The total number of detectable DDs for the case of uncorrelated component masses is an order lower than that for the case of a constant mass ratio distribution. This is seen from the fact that a binary system tends to have a more massive secondary for the case of a constant mass ratio distribution, and therefore more probably experiences two RLOFs during the evolution of the system.

The CE ejection efficiency $\alpha_{\rm CE}$ is another important parameter. A decrease in $\alpha_{\rm CE}$ leads to a decrease of the total number and the orbital periods of DDs, as seen from Tables 2 and 3 and Fig. 1. A binary system may merge more easily or have a shorter orbital period after suffering a CE phase with a smaller CE ejection efficiency.

The stellar wind velocity and the age or stellar formation period do not influence the results of Pop I very much. The change of stellar formation period from 15-0 Gyr (which means that stars are born between 15 and 0 Gyr ago) to 10-0 Gyr reduces the total number of detectable DDs by about 6 per cent. This means that the results of detectable DDs are more sensitive to the more recent stellar formation history. This is also true for Pop II.

For Pop II stars, I obtain similar results if I adopt similar model parameters. The birth rate of DDs from stable RLOF plus CE is higher for Pop II than for Pop I if I adopt the same stellar formation period. The range of radii for a Pop II star in the Hertzsprung gap is larger than that for a Pop I star with the same initial mass, thus the primary of a Pop II binary fills its Roche lobe more probably than a Pop I binary does in the Hertzsprung gap. A binary system with its Roche lobe filling primary in the Hertzsprung gap tends to have a stable RLOF process, and therefore stable RLOF plus CE plays a more important role for Pop II. The change of stellar formation period from 15-0 to 15-10 Gyr reduces the total number of detectable DDs by an order of magnitude, which means that the results of detectable DDs are more sensitive to the more recent stellar formation history.

The model parameters affect in a similar way the frequencies of WD binaries, CVs, DD mergers, SNe Ia, and the mergers of various types of DDs. A stronger stellar wind reduces all the frequencies. A higher mass transfer efficiency during stable RLOF increases the frequency of DD mergers and SNe Ia. For the case of uncorrelated component masses, I obtain a higher frequency of CVs but lower frequencies of SNe Ia and the mergers of DDs than for the case of a constant mass ratio distribution. A lower CE ejection efficiency reduces all the frequencies. All the frequencies are more sensitive to the more recent stellar formation history and all the frequencies are higher for Pop II than for Pop I if I adopt similar model parameters.

7.3 Expected birth rates and numbers of DDs, SNe Ia and CVs: comparison with observations

The frequencies and numbers quoted here, from Tables 2, 3 and 4, are based on the assumption that one binary with $M_1 \geq 0.8\,{\rm M}_\odot$ is formed annually in our Galaxy (e.g. Iben & Tutukov 1984a; Yungelson et al. 1993) for Pop I and Pop II.

The frequency of DD formation in our Galaxy ranges from 0.005 to 0.056 $\rm yr^{-1}$, the total number of DDs ranges from 20 to 266×10^6, while the total number of detectable DDs ranges from 0.5 to 3×10^6.

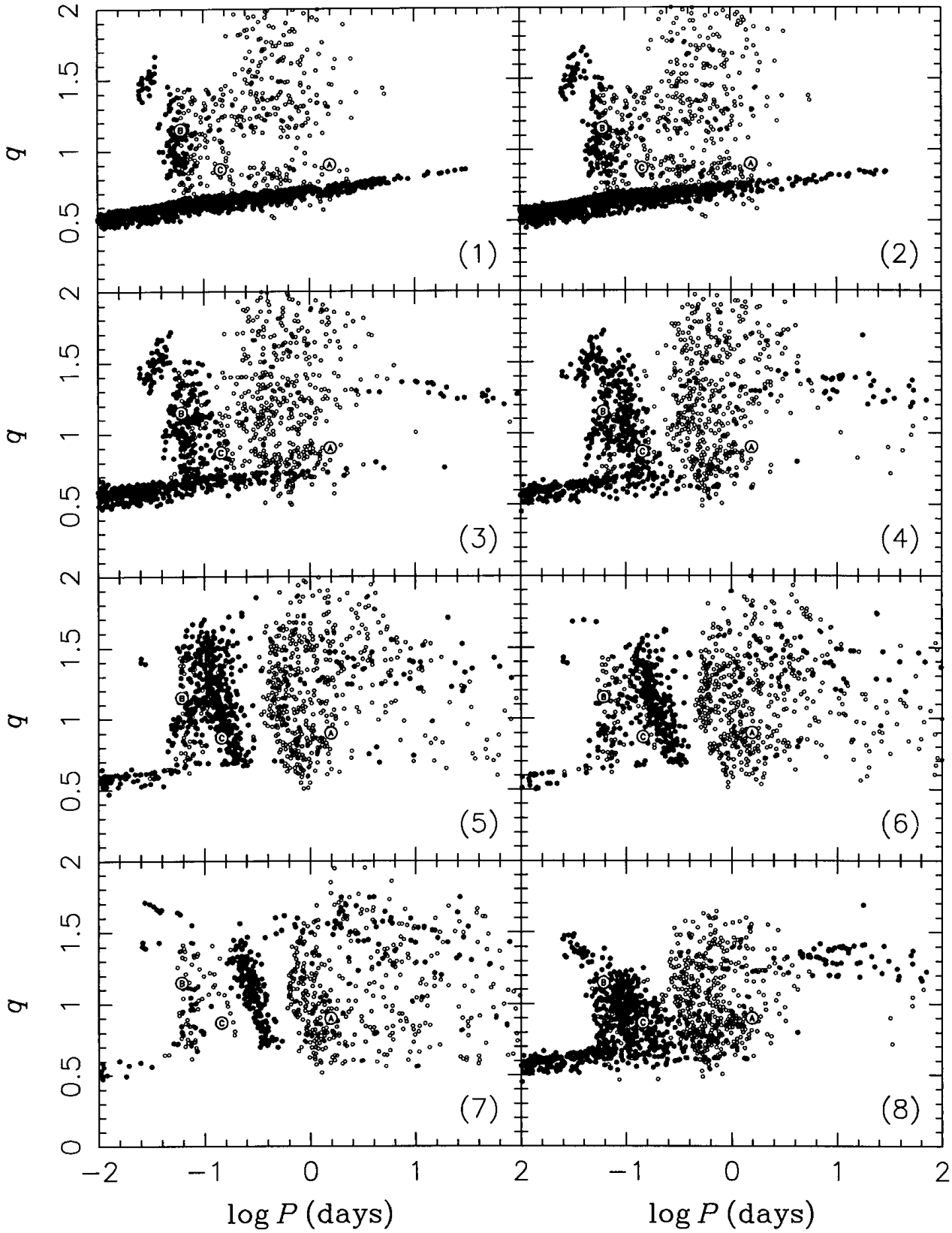

Figure 1. He+He DDs and CO+CO DDs with their brighter components detectable at present in our Galaxy in the plane (log$P$, q), where q is the ratio of the mass of the brighter component of a DD to that of the dimmer component ($q = m_{\rm brighter}/m_{\rm dimmer}$), P is the orbital period in days. (1)–(16) are for simulation sets 1–16. • stands for He+He DDs, and ∘ for CO+CO DDs.

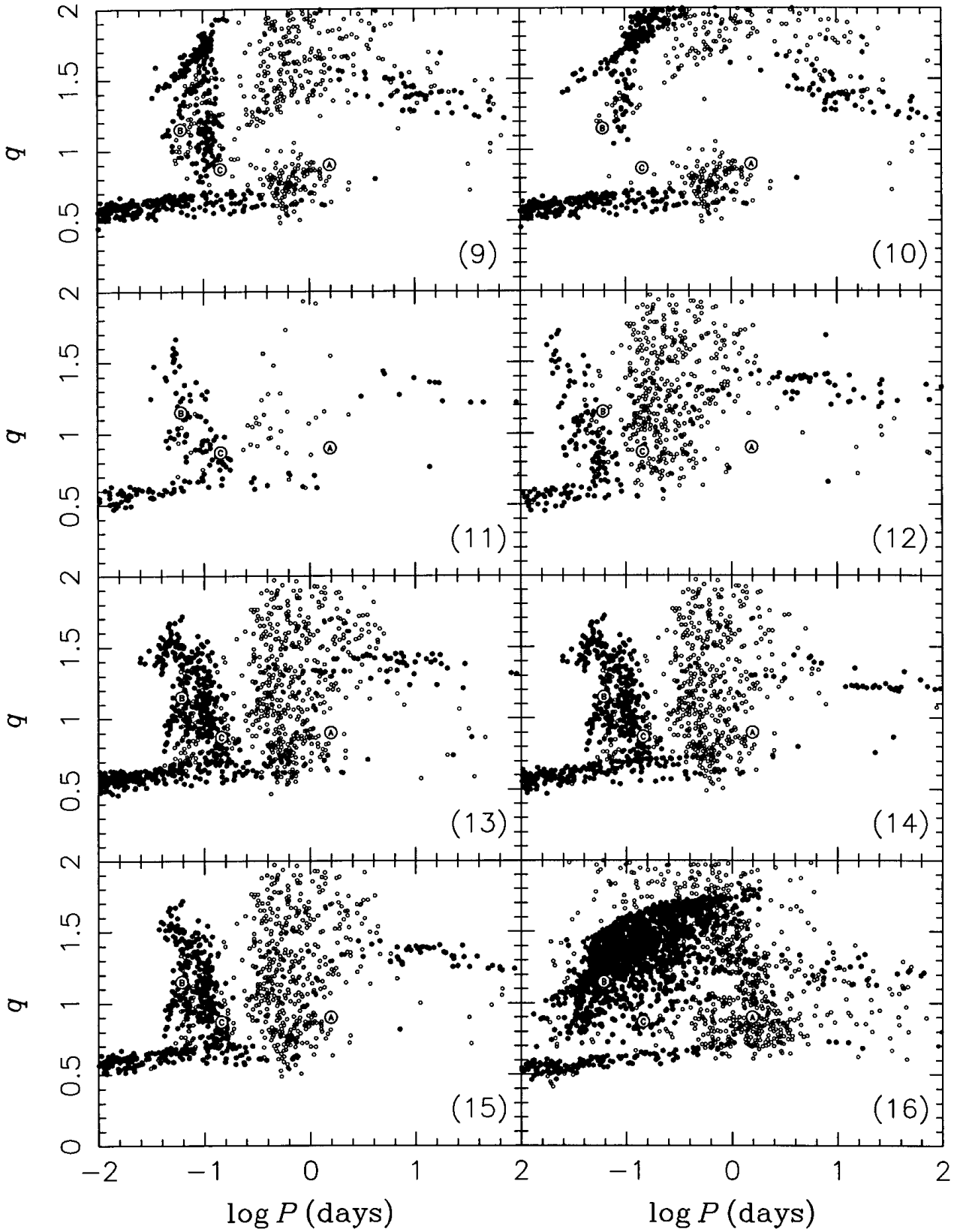

Figure 1 – *continued*

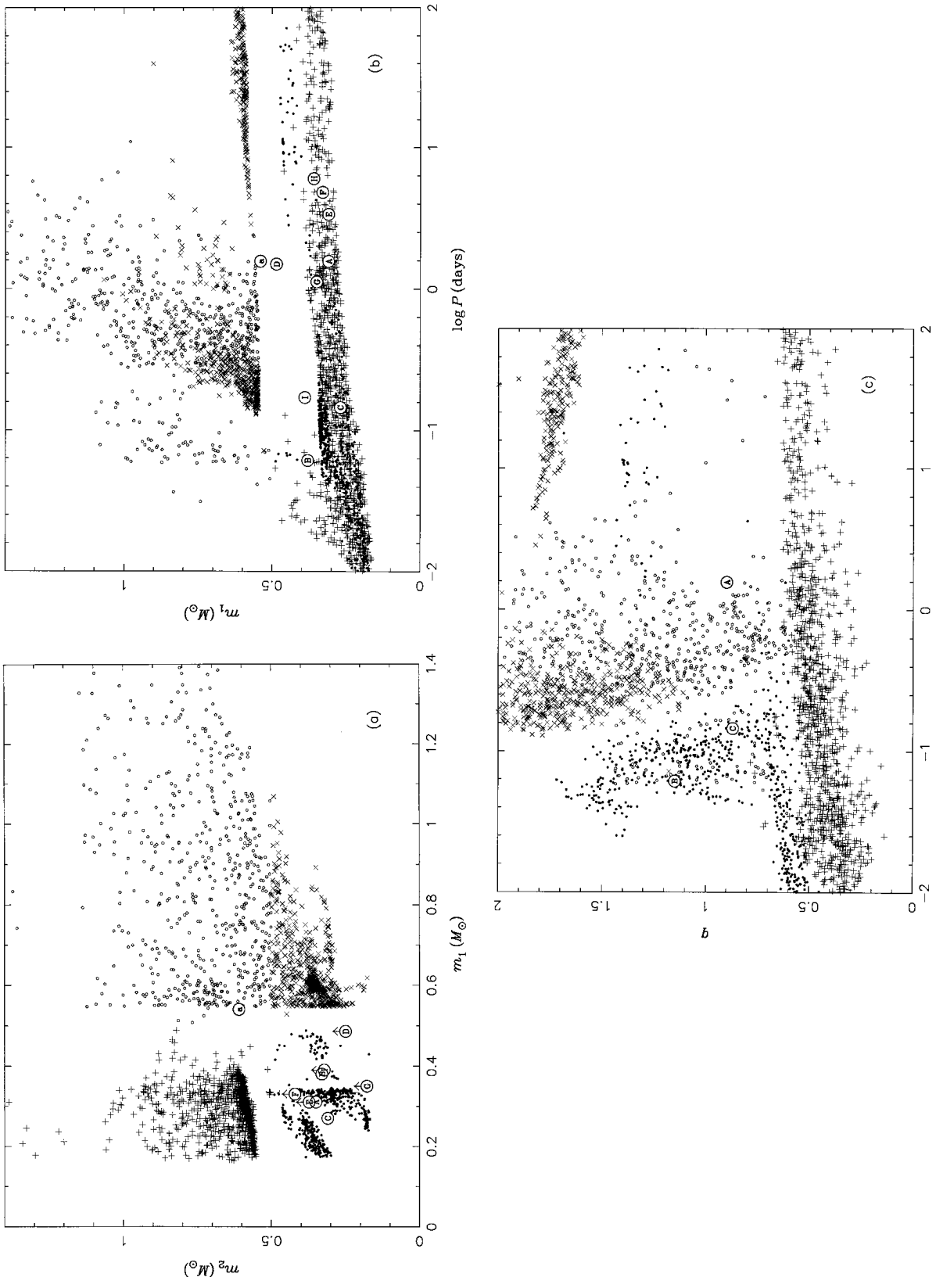

Figure 2. DDs with their brighter components detectable at present in our Galaxy for simulation set 4. (a) DDs in the plane of (m_1, m_2); (b) DDs in the plane of $(\log P, m_1)$; (c) DDs in the plane of $(\log P, q)$. m_1 and m_2 are the mass of the brighter component and the dimmer component of a DD, respectively, P is the orbital period and q is the mass ratio ($q = m_1/m_2$). •, +, ×, and ∘ stand for an He+He DD, an He+CO DD, a CO+He DD, and a CO+CO DD, respectively. Circled letters 'A' to 'I' are the observed DDs listed in Table 1, and circled letter 'a' refers to the same DD as 'A' does, but with component masses from Iben & Webbink (1989). An arrow above a circled letter denotes that the value of m_2 for a DD is a lower limit.

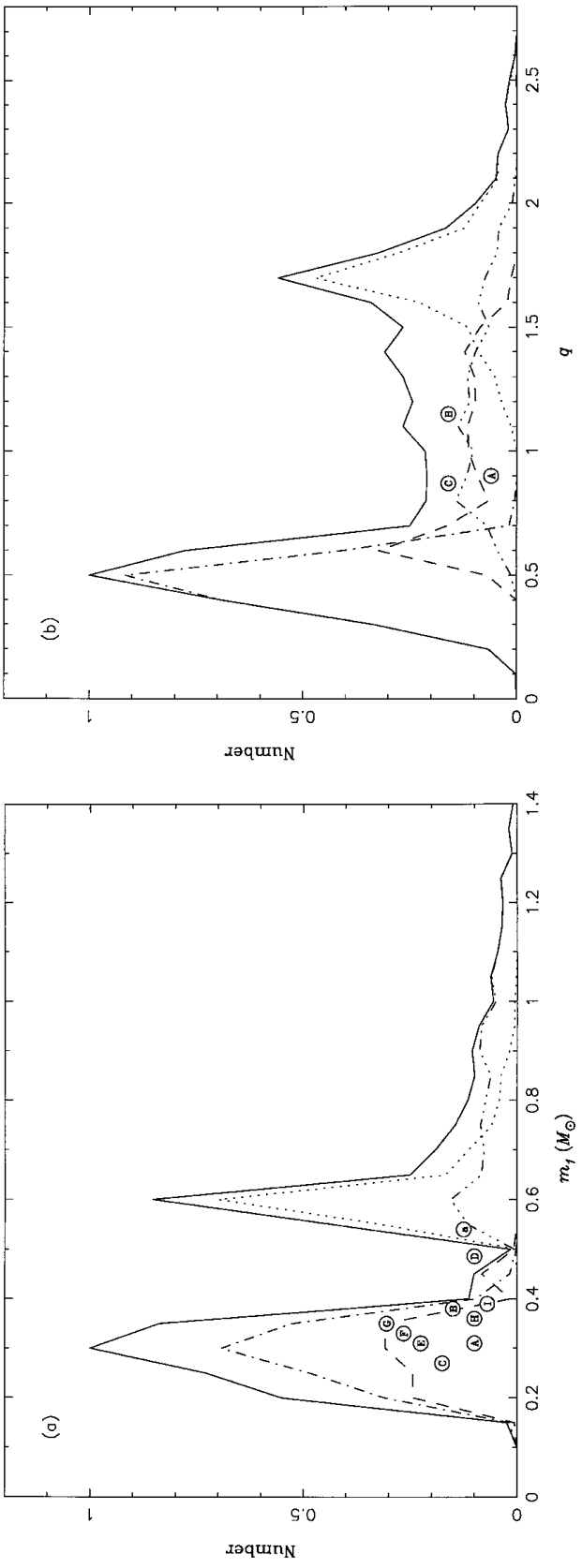

Figure 3. The distribution of primary (brighter component) masses (a), mass ratios of primary to secondary (b) and orbital periods (c) for DDs with their brighter components detectable at present in our Galaxy for simulation set 4. The solid curve is for all the detectable DDs, and dashed, dash–dot, dotted, and dash–dot-dot-dot curves are for DDs of He+He, He+CO, CO+He and CO+CO type, respectively. Circled letters 'A' to 'I' are the observed DDs listed in Table 1, and circled letter 'a' refers to the same DD as 'A' does, but with component masses from Iben & Webbink (1989).

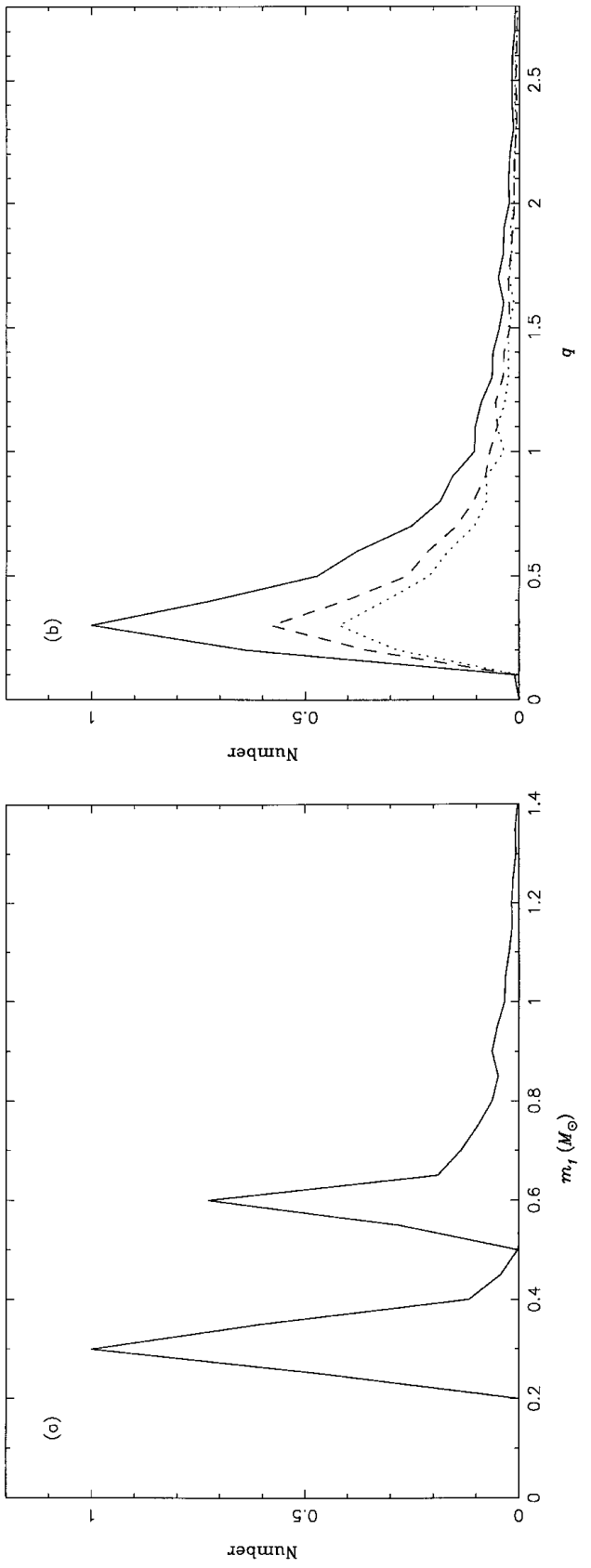

Figure 4. The distribution of WD masses (a), mass ratios of primary (WD) to secondary (b) and orbital periods (c) for post-CE systems at birth for simulation set 4. The solid curve is for all the systems at birth, and dashed and dotted curves are for post-CE systems with He WDs and CO WDs, respectively.

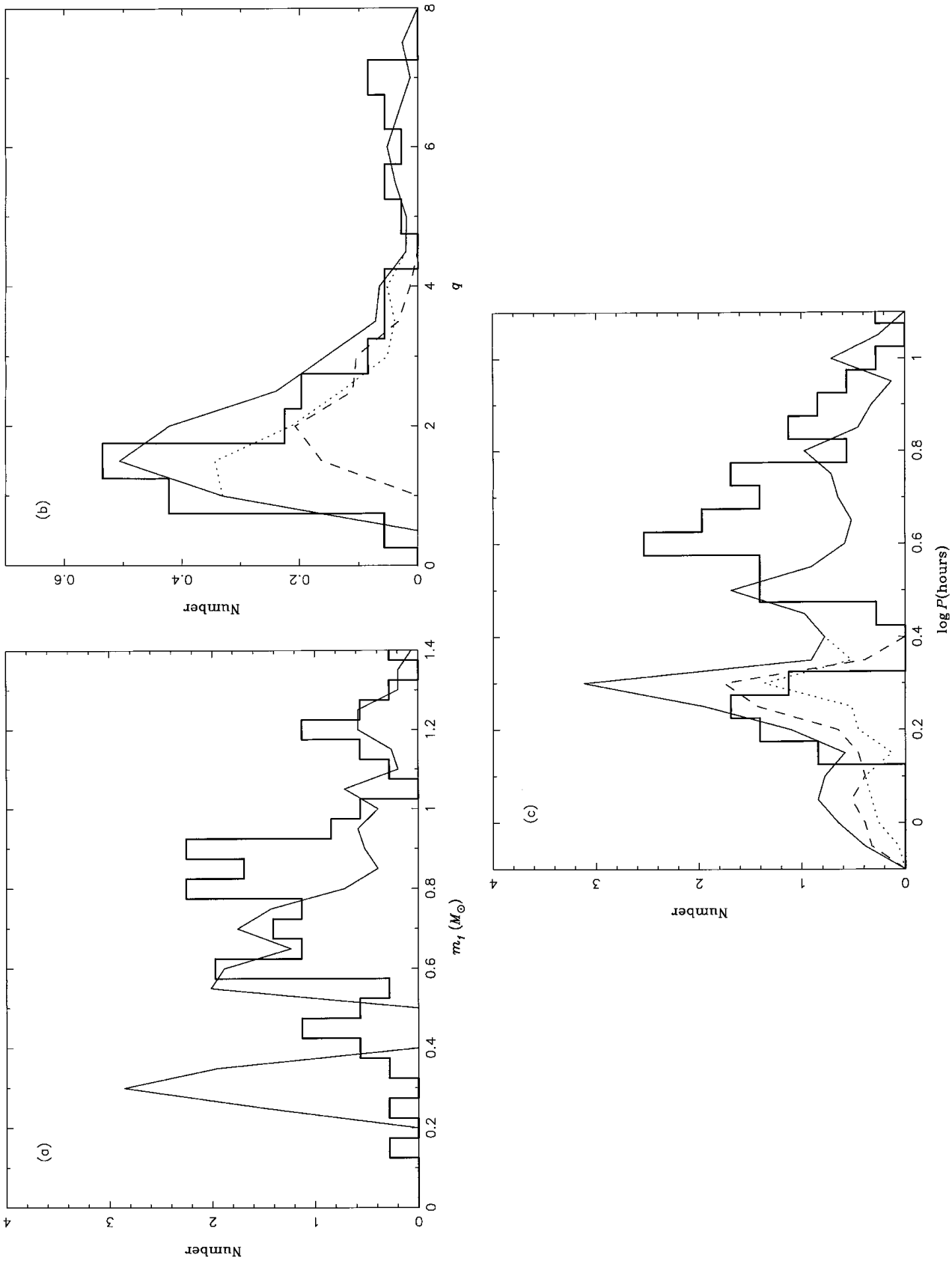

Figure 5. The distribution of WD masses (a), mass ratios of WD to MS star (b) and orbital periods (c) for CVs at birth for simulation set 4. The solid curve is for all the CVs at birth, and dashed and dotted curves are for CVs with He WDs and CO WDs, respectively. The histograms are for CVs observed (Ritter & Kolb 1995).

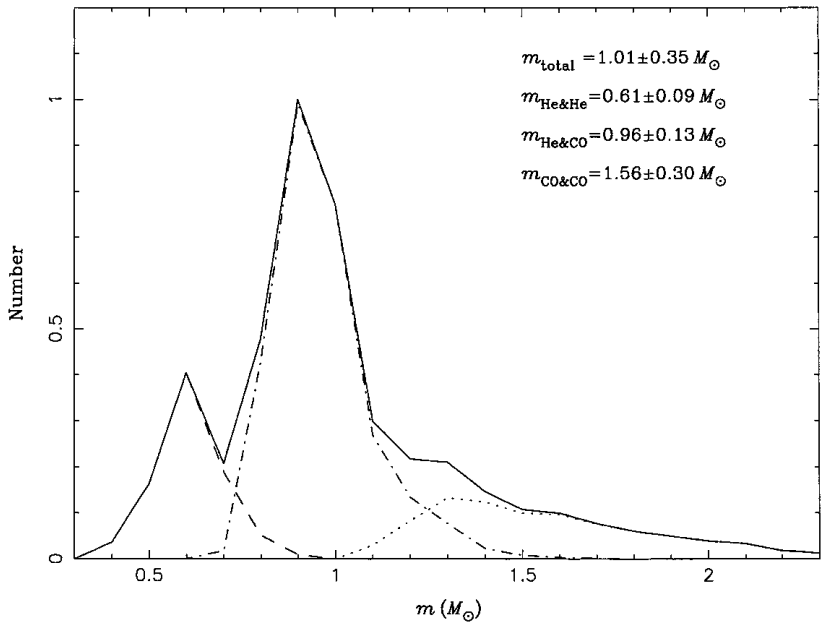

Figure 6. The distributions of masses of DD mergers at birth for simulation set 4. The solid curve is for all the mergers, and the dashed, dash-dot and dotted curves are for the mergers of two He WDs (sdO stars), the mergers of an He WD and a CO WD (R CrB stars), and the mergers of two CO WDs, respectively.

The birth rate of DD systems in my model is consistent with the upper limits (0.04–0.07) deduced from observations: for example $0.05{\rm yr}^{-1}$ (Robinson & Shafter 1987), or $0.04–0.07{\rm yr}^{-1}$ (Bragaglia et al. 1991).

The merger of two CO white dwarfs with a total mass larger than the Chandrasekhar limit may lead to a Type Ia supernova (Iben & Tutukov 1984a; Webbink & Iben 1987). The highest Type Ia supernova frequency for our Galaxy that we predict according to this model is $3.9\times10^{-3}{\rm yr}^{-1}$. This is consistent with the observational frequency estimated as $(3\text{-}4)\times10^{-3}{\rm yr}^{-1}$ by van den Bergh & Tammann (1991). For most of our simulations, the frequencies are in the range of $(3–4)\times10^{-3}\,{\rm yr}^{-1}$. The frequencies obtained in this paper are larger than those obtained in HPE2 and HEPT, in which planetary nebulae and barium stars and CH stars are mainly investigated. In HPE2 and HEPT, the merging time of DDs due to gravitational radiation is just a time-scale, as is the case in de Kool (1992). The time-scale is larger than the precise time I obtain from equation (4) in this paper.

The birth rate of CVs is 0.001 to $0.016{\rm yr}^{-1}$, depending heavily on the mass ratio distribution. The CV birth rate in our Galaxy is estimated by Ritter & Burkert (1986) to be about $10^{-14}\,{\rm pc}^{-3}\,{\rm yr}^{-1}$. By taking an effective Galactic volume of $5\times10^{11}\,{\rm pc}^3$, I convert my theoretical birth rate to obtain $(0.2–3.2)\times10^{-14}\,{\rm pc}^{-3}\,{\rm yr}^{-1}$, which is consistent with that of Ritter & Burkert. The birth rate obtained in this paper is again larger than those obtained in HPE2 and HEPT. A CV may be formed from a close white dwarf binary system after losing orbital angular momentum due to magnetic braking and/or gravitational radiation. In this paper, I use the angular momentum loss rate to obtain the precise formation time of a CV, rather than the time-scales (de Kool 1992) used in HPE2 and HEPT.

7.4 Choosing a good model: results from the model

The finding that mass ratios known for DDs are all around 0.9 or 1.1 has not been successfully explained in previous studies. Therefore the mass ratio problem is taken to be the main constraint to my models.

WD 0135−052, 0957−666 and 1101+364 have mass ratios of 0.9, 1.15 and 0.87 and orbital periods of 1.56, 0.061 and 0.1446 d, respectively. WD 0135−052 may be a DD of He+He type (both components are He white dwarfs), or a DD of CO+CO type (both components are CO white dwarfs), while both WD 0957−666 and WD 1101+364 are of He+He type. Therefore I plot DDs of both He+He and CO+CO type in the plane of mass ratio–orbital period for simulation sets 1–16 in Fig. 1. I also plot the three DDs observed in Fig. 1, in which letters 'A', 'B' and 'C' are used to represent WD 0135−052, 0957−666 and 1101+364, respectively. Both WD 0957−666 and 1101+364 should be located in the region of He+He DD, while WD 0135−052 should be located in the region of He+He DD, or in the region of CO+CO DD. As seen from Fig. 1, simulation sets 4, 8, 9, 11, 13, 14 and 15 are better at explaining the three DDs.

Simulation set 11 is discarded, since it gives too low frequencies of the formation of DDs and SNe Ia as compared with the observational ones. Simulation sets 4, 8 and 9 have different mass transfer efficiencies (0.25, 0.5 and 0.75, respectively) at stable

Figure 7. DDs with their brighter components detectable at present in our Galaxy for simulation set 4: (a) DDs from stable RLOF plus CE in the plane of (m_1, m_2); (b) DDs from stable RLOF plus CE in the plane of (log$P$, m_1); (c) DDs from stable RLOF plus CE in the plane of (log$P$, q); (d) DDs from CE plus CE in the plane of (m_1, m_2); (e) DDs from CE plus CE in the plane of (log$P$, m_1); (f) DDs from CE plus CE in the plane of (log$P$, q); (g) DDs from exposed core plus CE in the plane of (m_1, m_2); (h) DDs from exposed core plus CE in the plane of (log$P$, m_1); (i) DDs from exposed core plus CE in the plane of (log$P$, q). m_1 and m_2 are the masses of the brighter component and the dimmer component of a DD, respectively, P is the orbital period and q is the mass ratio ($q = m_1/m_2$). •, +, × and ∘ stand for DDs of He+He type He+CO type, CO+He type and CO+CO type, respectively. Circled letters 'A' to 'I' are the observed DDs listed in Table 1, and circled letter 'a' refers to the same DD as 'A' does, but with component masses from Iben & Webbink (1989). An arrow above a circled letter denotes that the value of m_2 for a DD is a lower limit.

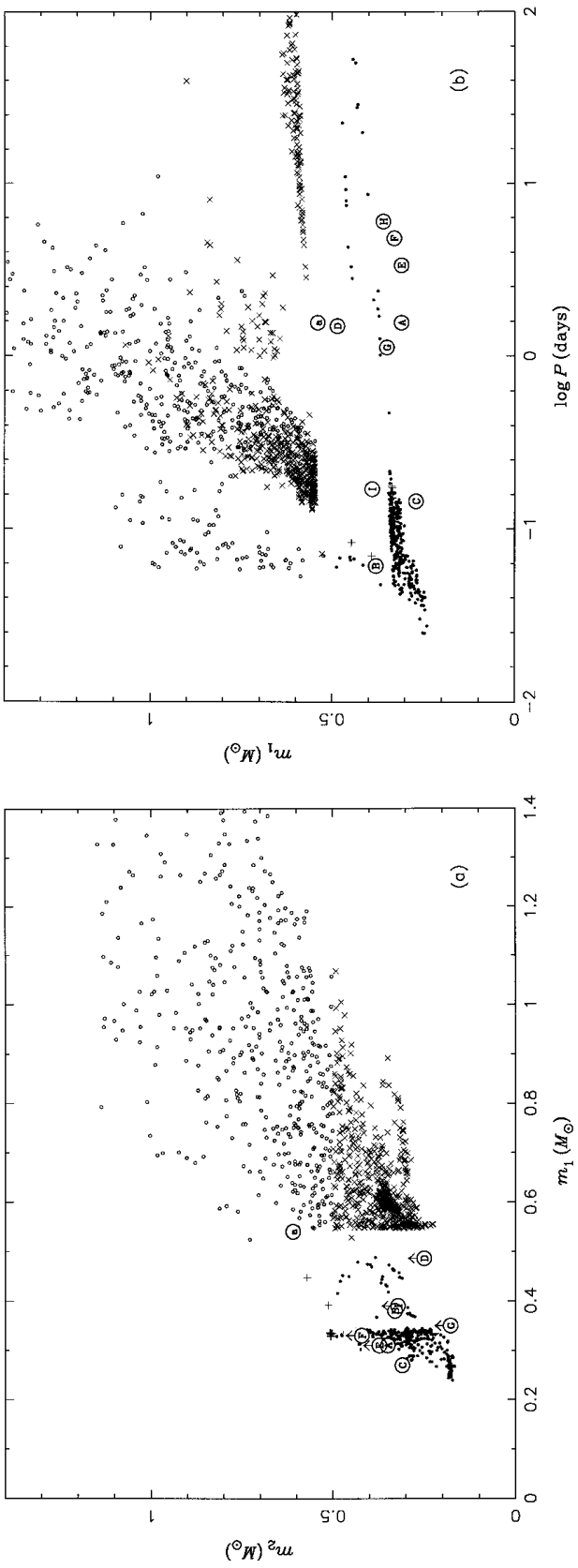

Figure 7. (a)–(c)

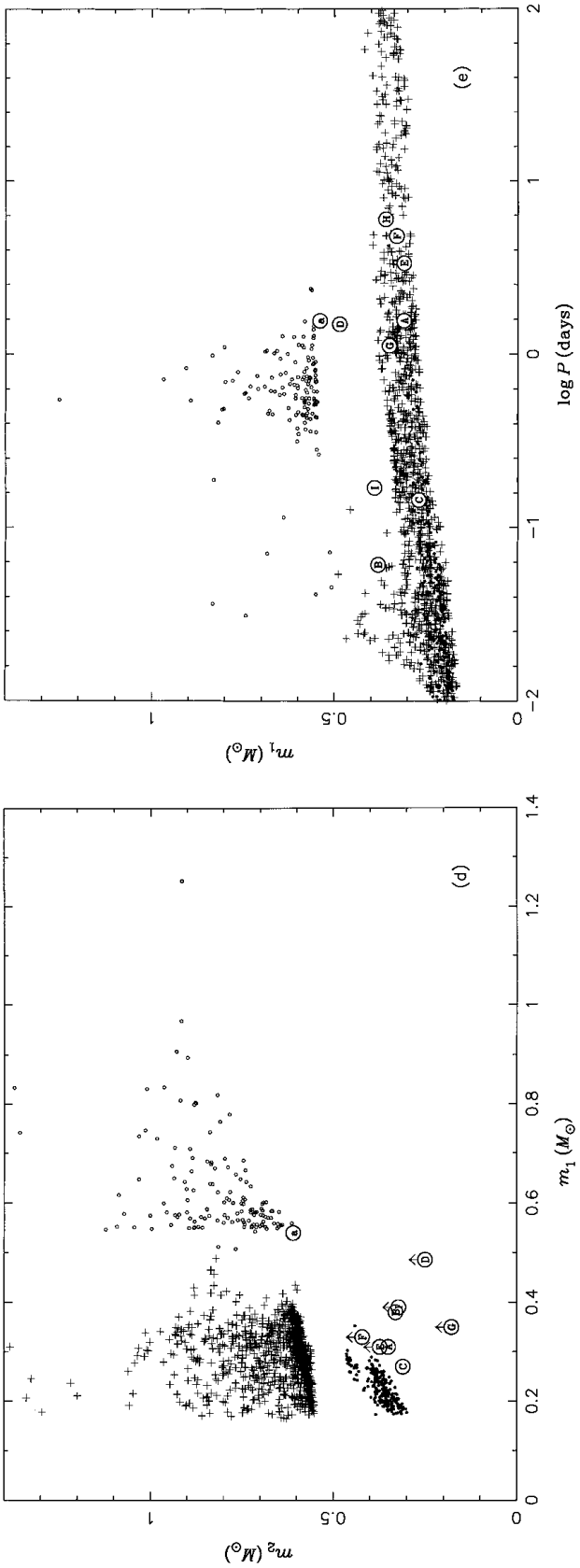

Figure 7. (d)–(f)

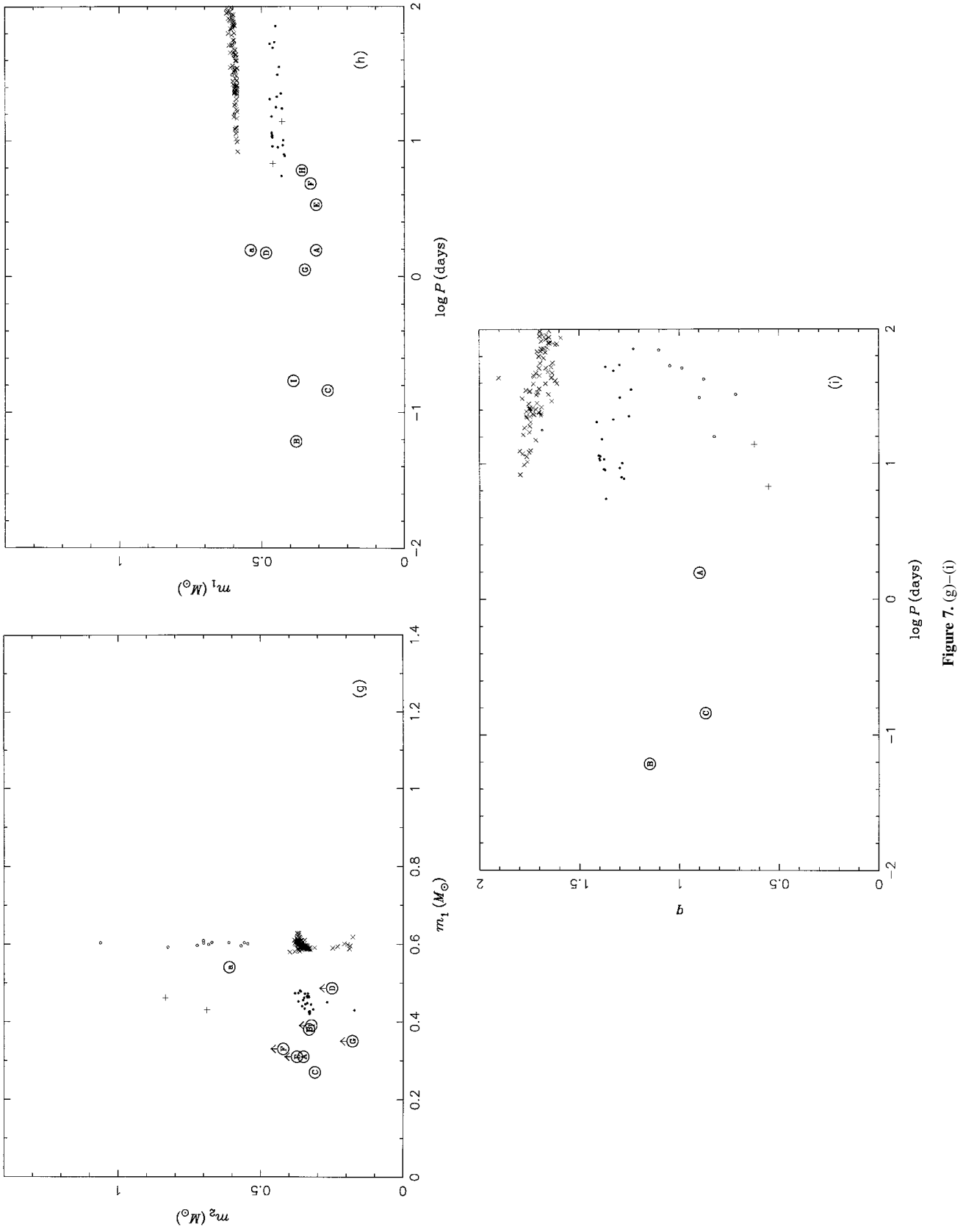

Figure 7. (g)–(i)

RLOF and are more or less equally good. A mass transfer efficiency of $\alpha_{\rm RLOF} = 0.5$ seems to be more reasonable (Paczyński & ZióÕkowski 1967; Refsdal *et al* 1974), and simulation set 4 is better than the sets 8 and 9 in this sense. Simulation sets 4, 13 and 15 have different wind velocities and are almost equally good. The mass-loss rate of the stellar wind is much stronger at the late stages of stellar evolution than at other stages, and a stellar wind velocity should be taken to be appropriate for stars at late evolutionary stages. Simulation set 4 has a stellar wind velocity $V_{\rm wind} = 20\,{\rm km\,s^{-1}}$, which seems to be more appropriate (Kwok 1982). Simulations 4 and 15 have different stellar formation periods (15-0 and 10-0 Gyr, respectively) and are almost equally good; the birth rate of CVs of set 4 is slightly closer to the observational one, and I just rather arbitrarily take simulation set 4 as better than simulation 15. Therefore I take simulation set 4 as the good model, and set 4 is used in the following discussions.

Note, however, that any of the simulation sets 4, 8, 9, 13, 14 and 15 could be chosen as the good model if a strong argument is found. The results of those simulation sets are similar.

As given from simulation set 4 (Tables 2, 3 and 4), the frequencies of stable RLOF plus CE, CE plus CE and exposed core plus CE are 0.014, 0.014 and 0.002 $\rm yr^{-1}$, respectively. The frequencies of the formation of DDs of He+He type, He+CO type, CO+He type and CO+CO type are 0.006, 0.011, 0.007 and 0.006 $\rm yr^{-1}$, respectively; the frequency of all DDs is $0.03\,\rm yr^{-1}$. The frequencies of white dwarf binaries (post-CE systems), DD mergers, the mergers of two He WDs (sdO stars), the mergers of He and CO WDs (R CrB stars), and the mergers of two CO WDs are 0.074, 0.029, 0.006, 0.018 and 0.006 $\rm yr^{-1}$, respectively. The local birth rate of CVs is $0.6\times10^{-14}\,\rm pc^{-3}\,yr^{-1}$, and the birth rate of SNe Ia is $3.6\times10^{-3}\rm yr^{-1}$. The birth rates of CVs, SNe Ia and all DDs are in very good agreement with the observations.

Simulation set 4 gives the total number of DDs in our Galaxy to be 1.8×10^{8}, and the number of detectable DDs to be 3.0×10^{6}. Stable RLOF plus CE contributes 46 per cent to the detectable DDs, CE plus CE contributes 48 per cent, and exposed core plus CE contributes 6 per cent. He+He DDs makes up 20 per cent of detectable DDs, He+CO DDs constitute 36 per cent, CO+He DDs 25 per cent and CO+CO DDs 19 per cent. The fraction of DDs with detectable He WDs is 56 per cent.

In the process of choosing the good model, one also sees that the models without a tidally enhanced stellar wind (simulation sets 1 and 2) and the model with conservative mass transfer during stable RLOF ($\alpha_{\rm RLOF} = 1$, simulation set 10) are not able to explain the mass ratios of WD 0957−666 and 1101+364.

7.5 The distribution for DDs: comparison with observations

I plot the detectable DDs from simulation set 4 and the observed DDs in the planes of (m_1, m_2), (log$P$, m_1) and (log$P$, q) in Fig. 2, where m_1 and m_2 are the masses of the brighter component of a DD and the dimmer component, respectively; P is the orbital period; and q is the mass ratio ($q = m_1/m_2$).

Fig. 2 explains the observation nicely by considering that the masses of white dwarfs cannot be determined precisely enough. WD 0135−052 is more likely to be a CO+CO DD rather than a He+He DD, as is shown by Fig. 2(c). The present calculation shows that 98 per cent of all DDs (including those undetectable) in the Galaxy have orbital periods larger than 1.5 h, and 79 per cent of detectable DDs have periods larger than 1.5 h. This means that DDs born with orbital periods smaller than 1.5 h may merge due to gravitational radiation as they cool to the undetectable state. Fig. 1 (panel 1) shows detectable DDs from simulation set 1, in which no stellar wind is considered. Simulation set 1 is not able to explain the mass ratio of WD 1101+364 and does not explain well enough the masses of the components of the observed DDs.

In Fig. 3, I also plot the distributions of masses of the brighter components of the detectable DDs, the distribution of mass ratios, and the distribution of orbital periods for simulation set 4. The distributions of masses and orbital periods explain the observation successfully, and that of orbital periods has a peak around 6 h. The distribution of mass ratios seems to have a problem. It has two peaks, one at 0.5 and one at 1.7, and a plateau between them. The observed three mass ratios (near unity) are located at the plateau. No mass ratios, however, have been observed at the two peaks. This may be due to observational selection effects. To detect the mass ratio of a DD requires a small difference between the luminosities (brightnesses) of the two components. A WD binary system (with an old WD) may experience a CE phase and may produce a DD. The CE phase may rejuvenate the old WD and the DD cools gradually after its formation. Both the rejuvenation and the cooling of a WD depend on its mass quite heavily, and the two components of a DD with a bigger mass difference may have a bigger luminosity difference. Therefore mass ratios far from unity will not be easily detected observationally. To make the argument more convincing, I need comprehensive models for the rejuvenation and the cooling of WDs, which are not available at present to my knowledge.

7.6 The distribution for close WD binaries and CVs

In Fig. 4, I plot the distributions of the masses of WDs (m_1), the mass ratios (q=m_1/m_2) and the orbital periods (log$P$) for close WD binary systems (post-CE systems) of simulation set 4. The distributions are for at birth and are almost the same as those for close WD binaries with the WD components detectable. Most of the WD companions are MS stars. Fig. 4 shows that the distribution of the masses has two peaks, one at $0.3\,{\rm M_\odot}$ and one at $0.6\,{\rm M_\odot}$. The distribution of the mass ratios has a peak around 0.3 and the distribution of the orbital periods has a peak around 1 d.

In Fig. 5, I plot the distributions of the masses of WDs (m_1), the mass ratios (q=m_1/m_2) and the orbital periods (log$P$) for CVs at birth for simulation set 4, together with the observational distributions from the CV catalogue of Ritter & Kolb (1995). Note that the newest version of the Ritter & Kolb catalogue (1997) will be available soon, though not currently available to me. Simulations and observations are marginally close, as one may see by considering the selection effect that CVs with lower WD masses are less easily observed due to their low luminosities. Fig. 5 shows that CVs with orbital periods larger than 2.5 h at birth always have CO WDs. By checking the CV catalogue, one sees that CVs with orbital periods larger than 4.7 h always have CO WDs rather than He WDs. By considering the uncertainty in the determination of the masses of WDs in CVs, I take my model as satisfactory.

7.7 The distribution for mergers of DDs

The angular momentum loss due to gravitational radiation may result in the coalescence of DDs. The distribution of the masses of the mergers at birth is plotted in Fig. 6. The distribution for all the mergers at birth peaks at $1.01 \pm 0.35\,{\rm M_\odot}$, that for the mergers of He+He DDs (sdO stars) peaks at $0.61 \pm 0.09\,{\rm M_\odot}$, that for the mergers of He+CO and CO+He DDs (R CrB stars) peaks at

$0.96 \pm 0.13\,M_\odot$, and that for the mergers of CO+CO DDs peaks at $1.56 \pm 0.30\,M_\odot$.

7.8 Possible formation scenarios for DDs observed

I plot the detectable DDs from each of the evolutionary channels of simulation set 4 and the observed DDs in the planes of (m_1, m_2), (log$P$, m_1) and (log$P$, q) in Fig. 7 in a similar way to Fig. 2.

One sees that WD 0957−666 and 1101+364 ('B' and 'C' in the figure) may be produced from the evolutionary channel of stable RLOF plus CE, since Figs 7(f) and (i) are not able to explain the mass ratios of WD 0957−666 or WD 1101+364 at all, and Fig. 7(c), which is for stable RLOF plus CE, explains the mass ratios of both DDs nicely. WD 0135−052 ('A' or 'a' in the figure) may be formed from the channel of stable RLOF plus CE or CE plus CE. The remaining DDs observed ('D', 'E', 'F', 'G', 'H', 'I' in Fig. 7) are more probably from the channel of CE plus CE when one takes into account the uncertainties in the determination of WD masses, and they are more possibly DDs of He+CO type. The possibility of these DDs being formed from stable RLOF plus CE and being He+He DDs should not be ruled out, however. Few He+CO DDs are produced from stable RLOF plus CE, since stable RLOF usually leaves a helium core with a mass less than $0.5\,M_\odot$, which evolves to an He WD rather than a CO WD.

7.9 Comparisons with the results of previous studies

Yungelson et al. (1994) studied the formation of SNe Ia. They gave a galactic birth rate of DDs of $0.087\,yr^{-1}$ in their standard model. In the good model of my present study, however, the birth rate is lower ($0.03\,yr^{-1}$). This is mainly because their standard model uses an α_{CE} that is actually higher than mine (see HPE2). As shown by Yungelson et al. (1994), a higher α_{CE} leads to a higher birth rate of DDs.

Han et al. (1995) studied the formation of planetary nebulae and close white dwarf binaries. They give the birth rate of DDs as $0.037\,yr^{-1}$, which is close to the result of the present study. Non-conservative stable RLOF evolution and stellar wind are considered in the present study but not in their study.

Iben et al. (1997) studied helium and carbon–oxygen white dwarfs in close binaries. The assumptions used in the present study are quite similar to theirs, and the results are quite similar too. Their standard model is more close to my simulation set 1 than to other sets in model assumptions. They give the birth rates of He+He semidetached systems and He+CO semidetached systems and SNe Ia as 0.01, 0.01 and $0.003\,yr^{-1}$, respectively. I give the birth rates as 0.011, 0.015 and $0.0029\,yr^{-1}$, respectively, in simulation set 1.

Fig. 1 of Iben et al. (1997) shows the distribution over white dwarf mass of helium and CO white dwarfs in close binaries. The distributions for helium white dwarf primaries and CO white dwarf primaries peak around 0.3 and $0.6\,M_\odot$, respectively. By comparing my Fig. 3(a) to the top panel of their fig. 1 and my Fig. 4(a) to the bottom panel of their fig. 1, I find that the positions of the peaks agree among each other, though their figure has a rather wide bin. I also find that their fraction of CO white dwarf close binaries is lower than mine; this is because I include thermal energy in the calculation of binding energy for envelopes of red giants. The thermal energy decreases the envelope binding energy for an AGB star more heavily than for an FGB star. Therefore a CE engulfing a CO core is more easily ejected in my calculation.

Figs 2(a) and (c) of Iben et al. (1997) give the distribution of orbital periods for DDs with helium WDs as primaries. By the combination of He+He and He+CO curves in Fig. 3(b) of the present paper, I find that the resulting curve is close to theirs. The shapes of the orbital period distribution for close WD binaries (the dashed and dotted curves in my Fig. 4c) are close to theirs (their fig. 3), though the population of close WD binaries of mine also contains those with MS secondaries more massive than $0.3\,M_\odot$.

The top panel of fig. 5 of Iben et al. (1997) shows the distribution of mass ratios for DDs. It is quite similar to Fig. 3(b) in this paper. The distribution has two peaks, the main one at $q = 0.5$ and the minor one at $q > 1$. Their bottom panel of fig. 5 shows the distribution of mass ratios for close white dwarf binaries. It peaks around $q = 1.5$, which is much higher than the peak $q = 0.3$ of Fig. 4(b) in the present paper. This is because their distribution is only for close white dwarf binaries with secondaries less massive than $0.3\,M_\odot$. As one may see, a less massive secondary leads to a higher mass ratio of primary to secondary.

8 CONCLUSION

(1) The model is successful in the explanation of birth rates of DDs, CVs and SNe Ia, and their birth rates are more sensitive to the more recent stellar formation history.

(2) The model satisfactorily accounts for the masses, mass ratios and the orbital periods of observed DDs.

(3) Stable RLOF plus CE and CE plus CE are the main evolutionary scenarios leading to the formation of DDs.

(4) The Galactic birth rate of DDs is $0.03\,yr^{-1}$, and the birth rate of DDs with He WDs as brighter components is $0.017\,yr^{-1}$.

(5) The number of detectable DDs in our Galaxy is 3×10^6, and DDs with brighter He WDs make up 56 per cent.

(6) The distribution of orbital periods of detectable DDs peaks around 6 h.

(7) The Galactic birth rates of close WD binaries, DD mergers, the mergers of two He WDs (sdO stars), and the mergers of He and CO WDs (R CrB stars) are 0.074, 0.029, 0.006 and $0.018\,yr^{-1}$, respectively.

(8) The mergers of two He WDs (sdO stars) and the mergers of He and CO WDs (R CrB stars) have masses of 0.61 ± 0.09 and $0.96 \pm 0.13\,M_\odot$, respectively.

(9) WD 0957−666 and WD 1101+364 are formed through the stable RLOF plus CE scenario.

(10) WD 0135−052 is more likely to be a CO+CO DD rather than a He+He DD

(11) CVs with longer orbital periods tends to have CO WDs.

(12) Mass transfer during stable RLOF is not conservative.

(13) A tidally enhanced stellar wind exists.

ACKNOWLEDGMENTS

This work is supported by the Pandeng Scheme and the Research Fund of Academia Sinica and Postdoctoral Research Fund of the Chinese Educational Commission. ZH thanks Dr Podsiadlowski of Oxford University for promoting discussion and making suggestions, and special thanks go to Dr Marsh of the University of Southampton for kindly providing the up-to-date observational DD list, and his suggestions. ZH also thanks the refree, Dr Sarna, for his valuable suggetions and comments.

REFERENCES

Althaus L. G., Benvenuto O. G., 1997, ApJ, 477, 313

Andersen J., 1991, A&AR, 3, 91
Bergeron P., Saffer R. A., Liebert J., 1992, ApJ, 394, 228
Bessell M. S., Brett J. M., Scholz M., Wood P. R., 1989, A&AS, 77, 1
Boffin H. M. J., Jorissen A., 1988, A&A, 205, 155
Boffin H. M. J., Paulus G., Cerf N., 1992, in Duquennoy A., Mayor M., eds, Binaries as Tracers of Stellar Formation. Cambridge Univ. Press, Cambridge, p.26
Boffin H. M. J., Cerf N., Paulus G., 1993, A&A, 271, 125
Bragaglia A., Greggio L., Renzini A., D'Odorico S., 1990, ApJ, 365, L13
Bragaglia A., Greggio L., Renzini A., D'Odorico S., 1991, in Woosley S.E., ed., Supernovae. Springer, New York, p.599
Castellani V., Degl'Innocenti S., Romaniello M., 1994, ApJ, 423, 266
De Greve J. P., 1993, A&AS, 211, 356
de Kool M., 1990, ApJ, 358, 189
de Kool M., 1992, A&A, 261, 188
Della Valle M., Livio M., 1996, ApJ, 473, 240
Eggen O.J., 1985, AJ, 90, 333
Eggleton P. P., 1971, MNRAS, 151, 351
Eggleton P. P., 1972, MNRAS, 156, 361
Eggleton P. P., 1973, MNRAS, 163, 279
Eggleton P. P., 1976, in Eggleton P. P., Mitton S., Whelan J., eds, Proc. IAU Symp. 73, Structure and Evolution of Close Binary Systems. Reidel, Dordrecht, p.209
Eggleton P. P., Faulkner J., Flannery B. P., 1973, A&A, 23, 325
Eggleton P. P., Fitchett M. J., Tout C. A., 1989, ApJ, 347, 998
Goldberg D., Mazeh T., 1994, A&A, 282, 801
Greenstein J. L., Sargent A. I., 1974, ApJS, 28, 157
Han Z., 1995, PhD thesis, Cambridge University
Han Z., Podsiadlowski Ph., Eggleton P. P., 1994, MNRAS, 270, 121 (HPE1)
Han Z., Podsiadlowski Ph., Eggleton P. P., 1995, MNRAS, 272, 800 (HPE2)
Han Z., Eggleton P. P., Podsiadlowski Ph., Tout C.A., 1995, MNRAS, 277, 1443 (HEPT)
Hjellming M. S., Webbink R. F., 1987, ApJ, 318, 794
Holberg J. B., Saffer R. A., Tweedy R. W., Barstow M. A., 1995, ApJ, 452, L133
Iben I., Jr, Tutukov A. V., 1984a, ApJS, 54, 335
Iben I., Jr, Tutukov A. V., 1984b, in Chiosi C., Renzini A., eds, Stellar Nucleosynthesis. Reidel, Dordrecht, p.181
Iben I., Jr, Tutukov A. V., 1993, ApJ, 418, 343
Iben I., Jr, Webbink R. F., 1989, in Wegner G., ed., White Dwarfs. Springer, New York, p.477
Iben I., Jr, Fujimoto M. Y., MacDonald J., 1992, ApJ, 388, 521
Iben I., Jr, Tutukov A. V., Yungelson L.R., 1997, ApJ, 475, 291
Kolb U., 1993, A&A, 271, 149
Kovetz A., Prialnik D., 1997, ApJ, 477, 356
Kroupa P., Tout C. A., Gilmore G., 1993, MNRAS, 262, 545
Kwok S., 1982, ApJ, 258, 280
Landau L. D., Lifshitz E. M., 1962, The Classical Theory of Fields. Pergamon, Oxford
Livio M., Soker N., 1984, MNRAS, 208, 763
Livio M., Soker N., 1988, ApJ, 329, 764
Marsh T. R., 1995, MNRAS, 275, L1
Marsh T. R., Dhillon V.S., Duck S.R., 1995, MNRAS, 275, 828
Mazeh T., Goldberg D., Duquennoy A., Mayor M., 1992, ApJ, 401, 265
Meyer F., Meyer-Hofmeister E., 1979, A&A, 78, 167
Miller G. E., Scalo J. M., 1979, ApJS, 41, 513
Moran C., Marsh T. R., Bragaglia A., 1997, MNRAS, 288, 538
Nomoto K., 1982, ApJ, 253, 798
Nomoto K., Iben I., Jr, 1985, ApJ, 297, 531
Paczyński B., 1976, in Eggleton P. P., Mitton S., Whelan J., eds, Proc. IAU Symp. 73, Structure and Evolution of Close Binary Systems. Reidel, Dordrecht, p.75
Paczyński B., Ziółkowski J., 1967, Acta Astron., 17, 7
Pastetter L., Ritter H., 1989, A&A, 214, 186
Pols O. R., Marinus M., 1994, A&A, 288, 475
Pottasch S. R., 1984, Astrophys. Space Sci. Library No. 107, Planetary Nebulae. Reidel, Dordrecht
Prialnik D., Kovetz A., 1995, ApJ, 445, 789
Rappaport S., Verbunt F., Joss P.C., 1983, ApJ, 275, 713
Refsdal S., Roth M. L., Weigert A., 1974, A&A, 36, 113
Reimers D., 1975, Mem. Soc. R. Sci. Liège, 6e Ser., 8, 369
Ritter H., Burkert A., 1986, A&A, 158, 161
Ritter H., Kolb U., 1995, in Lewin W. H. G., van Paradijs J., van den Heuvel E. P. J., eds, X-ray Binaries. Cambridge Univ. Press, Cambridge, p. 578
Ritter H., Kolb U., 1997, A&AS, in press
Robinson E. L., Shafter A. W., 1987, ApJ, 322, 296
Rogers F. J., Iglesias C. A., 1992, ApJS, 79, 507
Saffer R. A., Liebert J., Olszewski E. W., 1988, ApJ, 334, 947
Sarna M. J., Marks P. B., Smith R. C., 1996, MNRAS, 279, 88
Schulz H., Wegner G., 1981, A&A, 94, 272
Shara M. M., Prialnik D., Kovetz A., 1993, ApJ, 406, 220
Soberman G. E., Phinney E. S., van den Heuvel E. P. J., 1997, A&A, 327, 620
Sparks W. M., Stecher T. P., 1974, ApJ, 188, 149
Taam R. E., Bodenheimer P., 1989, ApJ, 337, 849
Taam R. E., Bodenheimer P., Ostriker J.P., 1978, ApJ, 222, 269
Tout C. A., Eggleton P. P., 1988, ApJ, 334, 357
Tout C. A., Hall D. S., 1991, MNRAS, 253, 9
van de Kamp P., 1971, ARA&A, 9, 103
van den Heuvel E. P. J., Bhattacharya D., Nomoto K., Rappaport S.A., 1992, A&A, 262, 97
van den Bergh S., Tammann G. A., 1991, ARA&A, 29, 363
van der Linden T. J., 1987, A&A, 178, 170
Verbunt F., Zwaan C., 1981, A&A, 100, L7
Webbink R. F., 1984, ApJ, 277, 355
Webbink R. F., 1988, in MikoÕajewska J., Friedjung M., Kenyon S. J., Viotti R., eds, The Symbiotic Phenomenon. Kluwer, Dordrecht, p.311
Webbink R. F., Iben I., Jr, 1987, in Philip A .G. D., Hayes D. S., Liebert J. W., eds, Proc. IAU Colloq. 95, The Second Conference on Faint Blue Stars. L. Davis Press, Schenectady, p.445
Weiss A., Keady J. J., Magee N. H., Jr, 1990, At. Data Nucl. Data Tables, 45, 209
Wesemael F., Winget D. E., Cabot W., van Horn H. M., Fontaine G., 1982, ApJ, 254, 221
Winget D. E., 1987, ApJ, 315, L77
Yungelson L. R., Tutukov A. V., Livio M., 1993, ApJ, 418, 794
Yungelson L. R., Livio M., Tutukov A. V., Saffer R. A., 1994, ApJ, 420, 336

This paper has been typeset from a T_EX/L^AT_EX file prepared by the author.